

Computational Aspects of Nitrogen-Rich HEDMs

Betsy M. Rice (✉) · Edward F. C. Byrd · William D. Mattson

U.S. Army Research Laboratory, AMSRD-ARL-WM-BD, Aberdeen Proving Ground,
Aberdeen, MD 21005-5069, USA
betsyr@arl.army.mil

1	Introduction	154
2	Computational Methods	156
3	Prediction of Properties of High-Nitrogen Solids (Neutrals, Ionics)	157
3.1	Performance Properties	158
3.1.1	Crystal Densities: Neutral Molecular Crystals	158
3.1.2	Crystal Densities: Ionic Molecular Crystals	163
3.1.3	Solid Phase Heats of Formation: Neutrals	166
3.1.4	Solid Phase Heats of Formation: Ionic Crystals	170
3.2	Prediction of Vulnerability and Environmental Hazard	176
4	Novel Polynitrogen Species	177
5	Novel High Pressure Phases of Nitrogen	178
6	Concluding Remarks	187
	References	187

Abstract A variety of computational procedures used to predict properties of energetic materials is presented. These procedures, based on standard atomistic simulation methods, demonstrate the ability to predict key properties of these materials related to performance or hazard. Several applications of the various methods for nitrogen-rich materials are provided to illustrate capabilities. Also, an overview of theoretical efforts in computational design of novel all-nitrogen materials is given.

Keywords Computational chemistry · Crystal density · Energetic materials · Heats of formation · Quantum mechanics

Abbreviations

A7	<i>Strukturbericht</i> designation for α -arsenic crystal lattice structure
B3LYP	Becke 3-parameter hybrid density functional using non-local correlation provided by Lee, Yang and Parr
BP	Black phosphorus crystal lattice structure. <i>Strukturbericht</i> designation is A17
CCSD(T)	Coupled cluster with single, double and perturbative triple excitations
CG	Cubic gauche
CHNO	Carbon-hydrogen-nitrogen-oxygenal

CSD	Cambridge Structural Database
DFT	Density functional theory
EM	Energetic material
ESP	Electrostatic potential
G2	Gaussian-2 theory for calculating total molecular energies
G3	Gaussian-3 theory for calculating total molecular energies
G3(MP2)	Variant of Gaussian-3 theory for calculating total molecular energies in which the basis set extensions are obtained at the second-order Møller–Plesset level
G3(MP2)//B3LYP	Variant of Gaussian-3 theory for calculating total molecular energies in which the geometries and zero-point energies are obtained from B3LYP density functional theory instead of those used in conventional G3 calculations
GGA	Generalized gradient approximation
GIPF	General interaction properties function
Gx	Variant of the G2 or G3 method
HEDM	High energy density materials
HF	Hartree–Fock
HPC	Hexagonally packed chain
MC	Monte Carlo
MD	Molecular dynamics
MM	Molecular modeling
MOLPAK	MOlecular PAcKing crystal structure prediction software
MP	Molecular packing
MP2	Second order Møller–Plesset theory
NVE	Microcanonical
NVT	Canonical
PES	Potential energy surface
QCISD(T)	Quadratic configuration interaction with single double and perturbative triple excitations
QM	Quantum mechanics
QMD	Quantum molecular dynamics
QSAR	Quantitative structure activity relationship
QSPR	Quantitative structure property relationship
RMS	Root mean square
WMIN	Lattice energy minimization software

1

Introduction

The development of accurate models and simulations of energetic materials (EM) has been aggressively pursued within the EM research community since the advent of computational capabilities. Numerous analytic and computational models that predict the performance of an EM in a variety of applications exist, but most have a significant dependence on empirical data that previously could be obtained only through measurement. Due to the cost and time associated with collection of such empirical data (i.e., synthesis

and testing), the EM community has recognized that for purposes of screening new materials, its dependence on such information must be reduced. Therefore, great attention has been given towards developing physics-based atomistic models for use in EM research and has resulted in a dramatic evolution of methods and applications of these to EM.

A variety of models based on atomistic simulation methods have been developed to predict key properties of an EM that are used to assess potential performance in a weapon or its sensitivity to impact [1, 2]. While showing a measure of success, these models still include some empiricism and have been developed for conventional explosives, most of which are composed of carbon, hydrogen, nitrogen, and oxygen (CHNO). Therefore, one cannot immediately conclude that the same models and methods will be applicable to the new class of high-nitrogen molecular and ionic crystals that are showing great promise as high energy density materials (HEDMs), and thus are limited in their use as screening tools. Also, concern for potential environmental hazards associated with the use and synthesis of EMs calls for the development of methods that will predict the environmental impact of any new material being considered for synthesis. Unfortunately, there are only a few methods that exist for such a purpose, both for CHNO and high-nitrogen materials, and significant efforts in development and assessment of such methods are still required. Efforts are being made to address all of these limitations, and will be discussed herein.

Atomistic methods in EM research are not limited to use as tools for screening purposes only. There are several examples where quantum mechanical characterizations of isolated molecules or elementary reactions are used to augment experimental information of newly synthesized high-nitrogen condensed phase materials [3–13]. Quantum mechanical approaches are also used to identify novel forms of nitrogen in which structural energy is stored, such as exotic all-nitrogen molecular species and high pressure polymorphic phases of solid nitrogen. Several examples will be discussed in this chapter. Atomistic simulation methods can also be used to predict probable reaction mechanisms and for exploring the dynamic response of a material to an initiating event. Simulations for the latter process using molecular dynamics (MD) methods, however, have been limited to conventional CHNO explosives and to our knowledge, only two have been performed for triazolium-based compounds, with a focus on predicting physical properties [14, 15]. Since there are no widespread applications of this methodology to high-nitrogen systems, these types of simulations will not be discussed in this chapter.

Section 2 will describe the various computational approaches used to develop predictive procedures for high-nitrogen solids. Section 3 will describe applications of these procedures to existing high-nitrogen HEDMs (both molecular and ionic crystals). Section 4 will be devoted to a discussion of predictions of novel all- or high-nitrogen species, followed by Sect. 5, in

which predicted non-molecular high pressure phases of solid nitrogen are presented. Section 6 will contain concluding remarks, including identification of needs for further advancement of predictive capabilities for this emerging class of EMs.

2 Computational Methods

Atomistic simulation approaches encompass a wide variety of methods that can be loosely categorized into three areas: methods based on 1) classical physics, 2) quantum physics, and 3) empirical models that use atomistic simulation results. The methods based on classical physics used in EM research include molecular modeling/molecular packing (MM/MP), molecular dynamics (MD), and Monte Carlo (MC). MM/MP applications in EM research are used mainly for ab initio crystal prediction, a method in which the most probable packing of a molecule in the crystalline state is predicted using information about a single molecule. The ab initio crystal prediction of densities of EM will be discussed in the next section. MC methods are used to predict thermodynamic properties, while MD simulations predict the time-dependent behavior of a material (although the results can also be used to predict thermochemical properties). The accuracy of results using any of these methods is almost completely dependent on the quality of the description of interatomic interactions within a system. While some promising interaction potentials have been developed and successfully used in MC or MD simulations of conventional CHNO EMs [16–19], we are unaware of similar simulations for high-nitrogen HEDMs. Therefore, our discussion of simulation methods based on classical physics will be limited in this chapter.

Quantum mechanical methods are widely used in research of high-nitrogen energetic materials; applications include the evaluation of elementary reactions, establishing stability rankings among possible conformers or the generation of molecular properties, such as equilibrium structures, vibrational spectra, electrostatic potentials (ESP), electron densities, and thermodynamic information. Various QM theories ranging from the highly accurate CCSD(T) method to more computationally tractable approaches [such as density functional theory (DFT) or second-order perturbation theory (MP2)] have been applied to prediction of various molecular properties, many of which will be discussed in the next section. Most calculations using the extremely accurate quantum mechanical methods are performed to characterize all nitrogen molecules (Sect. 4), determine stability, and, in the case of species that are not stable, computationally design derivatives that will generate a stable species. Many of these studies have been limited to a small number of atoms, due to prohibitive computational requirements associated with high levels of quantum mechanical theory. Less accurate approaches

(i.e., DFT using modest basis sets) have been used for predicting molecular properties associated with screening since these can be calculated for large molecules rapidly yet provide sufficiently accurate results. Atomistic simulation of novel high pressure phases of nitrogen has been dominated by solid state DFT treatments, the only computationally tractable quantum mechanical method for the condensed phase. These calculations will be reviewed in Sect. 5. Although there are numerous classical molecular simulations of highly compressed nitrogen, none of the interaction potentials used in those simulations correctly model phase transitions occurring in the nitrogen system and will not be discussed herein.

QM methods are also used in the third category of atomistic simulation methods we will include in this discussion. We focus on quantitative structure activity relationship/quantitative structure property relationship (QSAR/QSPR), a computational chemistry methodology that is extremely popular within the pharmaceutical community for new drug design. This approach establishes mathematical correlations between molecular descriptors (an inherent property of the chemical system) and various physico-chemical properties and behavior for various classes of compounds. An extensive compilation and description of over two thousand molecular descriptors are provided by Todeschini and Consonni [20]. While many of the descriptors are empirically derived or obtained from experimental information, many of them can be generated using quantum mechanical methods [21]. QSPR/QSAR methods using conventional and quantum-mechanical molecular descriptors have been used successfully to predict certain key properties of EMs for conventional CHNO materials [1] and applications will be described in the next section. Drawbacks to this method are its empiricism and reliance on experimental information; predictive capability of this method is not ensured for systems that are outside of the data set to which the QSPRs were parameterized. As with all empirical models, there is a possibility that a QSPR will perform poorly for dissimilar chemical systems. To our knowledge, this approach has not been widely applied to high-nitrogen materials.

The theoretical methods that will be discussed in this chapter represent only a subset of the various atomistic simulation methods used in computational materials research, and we refer the interested reader to the various comprehensive reviews on each method [22–30]. For the purposes of this chapter, however, we will highlight important points associated with various theories in application to the high nitrogen materials.

3

Prediction of Properties of High-Nitrogen Solids (Neutrals, Ionics)

The majority of efforts in developing predictive capabilities have focused on calculating properties that are indicative of the performance of a material. In

recent years, however, vulnerability requirements and environmental restrictions have demanded that these factors be given equal or greater weight in the development and design of new materials, thus facilitating development of predictive models to address these aspects. In this section, we will describe the various models and methods used to predict these properties, and various applications to high-nitrogen HEDMs.

3.1

Performance Properties

Special attention has been given to the prediction of two properties that are used to provide an initial assessment of the potential performance of a material in a gun or warhead: the heat of formation and the density of the material. A variety of computational chemistry methods to accurately predict such performance properties [1, 31] exists, but applications to EM have been limited almost exclusively to conventional CHNO explosives. Unfortunately, there has been no similar wide-scale application of these computational methods to high nitrogen compounds. Additionally, there have not been extensive applications to ionic crystals (either high-nitrogen or CHNO salts), since the majority of EMs are neutral molecular organic crystals. Previous tools that have been developed to predict either of these properties for CHNO energetic neutral crystals are not suited for ionic materials, as will be described hereafter. Further, applications of existing tools that work well for CHNO neutral molecular crystals have shown inconsistent (and sometimes poor) behavior when applied to high nitrogen materials. Thus, the existing methods must be reassessed and modified to accommodate the high nitrogen systems, and alternative methods should also be explored. In this section, we will present some of these alternatives.

3.1.1

Crystal Densities: Neutral Molecular Crystals

We will begin this section with a discussion of the prediction of crystal densities for neutral molecular crystals. Several approaches have been used to predict crystal densities without a priori knowledge of the system. The first, and most sophisticated, is that of *ab initio* crystal prediction, in which the crystal microstructure is determined using information about a single, isolated molecule. While a number of procedures have been developed and assessed [32], all methods generally follow a three-step computational approach. The first step corresponds to generating a three-dimensional model of the molecule (the packing moiety) that will be used to construct candidate crystals of different symmetries. In the next step hypothetical crystal structures using the molecular models are created; the contents of the structures are dependent upon the crystal symmetry being explored and the orienta-

tion of the packing moiety. In the third step the energy of each hypothetical crystal is minimized with respect to lattice and molecular orientation parameters. After generating a large series of candidate crystal structures, the crystals can then be ranked (usually by energy or density). Although it has been shown to be a very useful predictive methodology, it suffers from certain limitations. The majority of computational methods assume that the crystal structure with the lowest lattice energy corresponds to the thermodynamically favored structure rather than the structure with the lowest free energy. This assumption effectively ignores entropic and vibrational enthalpic contributions to the free energy and does not consider kinetic factors associated with crystal growth, such as solvent effects and crystallization conditions. Another of the major limitations of this method of crystal density prediction is its reliance on a description of interatomic interactions. As in any atomistic modeling procedure, the quality of the result is dependent on the accuracy of the description of the interatomic forces. Finally, current methods require significant improvement in their search methods used to generate the candidate crystals, particularly for systems in which the asymmetric unit of a crystal (Z') is greater than one [32]. However, the utility of the procedure in EM research has been demonstrated, in spite of the aforementioned assumptions and limitations [33, 34]. A survey study [34] was performed in which 174 CHNO molecular crystals whose molecules contained functional groups common to CHNO explosives (i.e., nitramines, nitroaliphatics, nitrate esters, and nitroaromatics) were subjected to the method of ab initio crystal prediction using a transferable CHNO interaction potential [19] and the method developed by Ammon and co-workers (MOLPAK/WMIN) [33]. The systems chosen were restricted to crystalline space groups and systems that could be treated by MOLPAK/WMIN (i.e., $Z' \leq 1$). The study showed that for 85% of the chemical systems simulated, the method and model produced a crystal structure whose lattice parameters and contents of the crystal (i.e., molecular positions and orientations) matched the experimental crystal. Additionally, approximately 75% of these were the low energy structures of all possible candidates generated in the crystal prediction process. Predicted densities (calculated at 0 K) had a root-mean-square (rms) deviation from experiment of 3%. Inclusion of thermal effects is expected to bring these results more in line with the experimental values. This study showed that the method of ab initio crystal prediction is suitable to predict crystal densities of a new EM (provided the description of the interatomic interactions are reasonably accurate). However, because it utilizes an empirically derived interatomic model that was parameterized to CHNO systems, it cannot be assumed that the model will adequately predict structures of systems that are dissimilar from the original set to which it was parameterized. We demonstrate this in an application of the same interaction potential [19] and the method of ab initio crystal prediction to six high-nitrogen neutral molecular crystals synthesized by Klapötke [35]. The results were unsatisfactory; in

three cases the experimental crystal was not found among the various polymorphs that were generated in the calculations. For the remaining three, two of the structures identified as matching the experimental crystals were significantly higher in energy than those of other polymorphs generated in the calculations. Furthermore, the contents of the unit cells and the cell dimensions had unacceptably large deviations from the measured values. This exercise clearly demonstrated a need for an interaction potential to treat such high-nitrogen compounds. Ammon has recently refined the default interatomic interaction potential used in the MOLPAK/WMIN suite of programs to describe high-nitrogen systems [36]. Application of the MOLPAK/WMIN methods and this newly refined interatomic potential produces densities of eight high nitrogen crystals within a few percent. These results are given in Table 1. Further assessments of this model and method for high-nitrogen systems are being performed as experimental information is being collected.

Ab initio crystal prediction provides a density value and important information about the positions of the atoms in the unit cell, invaluable information that can be used to construct molecular models for use in other simulations or might be useful in analysis of experimental results of dynamic response (e.g., directional shock sensitivity). Unfortunately, the methods are computationally intensive and analysis of the results is not trivial. For assessment of potential performance, often the user only needs the value of the crystal density at room conditions. For such calculations, QSAR/QPSR approaches are extremely attractive due to their ease of use and speed. Several QSPR-type approaches have been used to predict condensed phase densities of molecular organic systems [37–45]; some of which are included in EM research. In some of the QSPR-type approaches, a property called “molecular

Table 1 Crystal densities predicted using molecular volumes within the 0.001 a.u. isosurface of electron density

System	Expt	MOLPAK/ WMIN [36]	6-31G**		6-311+G(2df,2p)	
			0 K	Temperature corrected	0 K	Temperature corrected
g088 [35]	1.473	1.44	1.462	1.436	1.423	1.398
gn085 [35]	1.381	1.33	1.335	1.313	1.290	1.269
Mincob [224]	1.515	1.484	1.524	1.500	1.473	1.449
weig1a [35]	1.444	1.491	1.488	1.453	1.440	1.406
g098 [35]	1.515	1.479	1.489	1.462	1.441	1.415
g096 [35]	1.522	1.495	1.555	1.527	1.504	1.476
Jahxog [225]	1.719	1.766	1.686	1.646	1.635	1.596
Iceduq [226]	1.384	1.423	1.382	1.349	1.345	1.314
Average % deviation		- 0.4	- 0.3	- 2.2	- 3.3	- 5.2
Rms % deviation		2.7	2.0	2.9	3.9	5.6

volume” is used in the development of the QSPR. The concept of molecular volume is ambiguous and can be defined in a variety of ways. For example, the experimental molecular volume in the Cambridge Structural Database (CSD) [46] is defined as the ratio of the volume of a unit cell to the number of molecules within the cell. Molecular volume can also be approximated assuming group or atom additivity,

$$V_{VA} = \sum n_i V_i, \quad (1)$$

where V_{VA} is the molecular volume assuming additivity, V_i is the volume of the i^{th} constituent atom or functional group, and n_i is the number of the i^{th} atoms or functional groups contained within the molecule. The atomic or group volumes can be defined by parameterizing to a large set of experimental crystal data [41, 43, 47, 48], or can be derived using accepted standard values, such as van der Waals radii [45]. Density predictions [39, 40, 44] have also been made using the general interaction properties function (GIPF) methodology [49–51], developed by Politzer for quantum-mechanical-based QSPR-like applications to predict macroscopic properties of a variety of materials. In this methodology, a GIPF is a function that uses statistical descriptors of the electrostatic potential (ESP) mapped onto a molecular surface to describe some macroscopic property. The parameters of the GIPF are determined by fitting to experimental information. In all of these calculations, the molecular surface is defined to be the 0.001 electrons/bohr³ isosurface of electron density [52]. In addition to the statistical descriptors of features of the surface ESP, Politzer frequently uses the area of the molecular surface in his GIPFs [49–51]. Politzer and co-workers developed GIPFs to predict liquid and crystal densities for numerous compounds [44]; the crystal density GIPF was a function of the area of the molecular surface and the variance of the surface ESP, where the electron density ESPs were calculated at the HF/STO-3G level. These authors indicated that this GIPF could be modified to use molecular volume rather than surface area, but that the resulting GIPF was sufficiently accurate to render such a calculation unnecessary. Subsequent studies using the GIPF approach for crystal density prediction [39, 40, 45] showed improvement upon replacing the surface area term with molecular volume, defined as either the volume contained within the molecular surface used in the Politzer approach [39, 40] or the van der Waals volume [45]. Pan and Lee showed that the original Politzer GIPF for crystal density prediction was not transferable to cyclic and caged compounds (many of which included EMs), and required reparameterization to produce acceptable results [40]. Additionally, Bouhmaida and Ghermani, who used experimental electron densities in generating the surface ESPs, found that the volume within the molecular surface was adequate for predicting crystal density, and that the surface variance was a poor descriptor in establishing this correlation [39]. They concluded that the differences between the results generated by Politzer [44] and their

application might be due to alterations of the ESPs of the molecules when in the solid state.

We have undertaken a study in which molecular volume is used to predict crystal densities for 181 CHNO species for which experimental crystallographic information exists. In this study, we defined our molecular volume to be that contained within the 0.001 a.u. isosurface of electron density of a molecule calculated at the B3LYP/6-31G** level. This level of QM theory is somewhat of an improvement over that used by Politzer and Murray [44] and Pan and Lee [40]. Two sets of molecular volumes were generated: one set was composed of volumes corresponding to the molecules in configurations consistent with those of the experimental crystals (denoted V_{Expt}), and the other (V_{opt}) was composed of molecules in equilibrium gas phase configurations (optimized at the B3LYP/6-31G** level). Since the geometry optimizations produce a 0 K result, we imposed a thermal correction to each system. This correction assumes isotropic expansion and has the form

$$V_{\text{opt,Corrected}} = V_{\text{opt}}(1 + \alpha T), \quad (2)$$

where T denotes the temperature at which the crystal structure was measured and α was determined by fitting the right-hand side of Eq. 2 to the experimental molecular volumes (as defined earlier in [46]). For the set of molecules whose configurations correspond to the experimental structure, thermal and crystal field effects are already included; therefore, no thermal correction was imposed on molecular volumes or densities calculated using these structures.

V_{Expt} and V_{opt} were then compared with experimental values; molecular volumes calculated using experimental structures had average and rms deviations from experiment of -4.2 and 5.8% , respectively. This corresponds to 6.3% rms deviation in crystal density. Average and rms deviation of V_{opt} from experiment are -0.9 and 3.7% , respectively. Application of the thermal correction to V_{opt} produced average and rms deviations from experiment of 1.3 and 3.8% , indicating thermal effects are minimal. These V_{opt} correspond to a 3.6% rms deviation from experiment in crystal density, indicating far better agreement with experiment than results using the molecular configuration corresponding to the measured crystal structure. The maximum deviations of molecular volume and density from experimental results from this set are 42.8 \AA^3 and 0.166 g/cc , respectively. We note that this method of crystal density prediction produced statistical agreement with experiment as good as those generated in the study of 174 CHNO systems using ab initio crystal prediction [34], at a substantially reduced computational cost. However, we emphasize that this method does not provide any information about the arrangement of the atoms within the unit cell.

We next calculated molecular volumes for eight high-nitrogen neutrals using two different basis sets [6-31G** and 6-311+G(2df,2p)] and the B3LYP density functional to explore the effect of basis set size on the molecular vol-

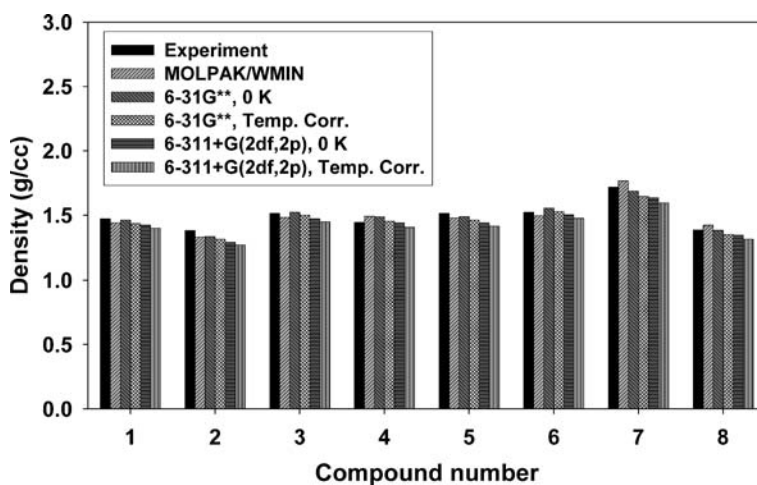


Fig. 1 Comparison of densities of high-nitrogen EM crystals (g/cc) using experimental crystal densities, MOLPAK/WMIN predictions, direct evaluation of 0 K and temperature-corrected molecular volumes using the 6-31G** basis set, direct evaluation of 0 K and temperature corrected molecular volumes using the 6-311+G(2df,2p) basis set

ume. In this study, geometries were optimized at the B3LYP/6-31G** level. Densities calculated using molecular volumes within the 0.001 a.u. isosurface of electron density with and without the temperature correction described above are listed in Table 1; a visual comparison with experimental values is given in Fig. 1. Additionally, results generated by Ammon using the recently modified force field (described earlier) and the MOLPAK/WMIN procedure [36] are also shown in Fig. 1. Temperature-corrected and 0 K crystal densities calculated using the larger basis set both have larger percent deviations from experiment than the other theoretical treatments. The MOLPAK/WMIN predictions (temperature corrected using factor recommended by Hoffman [41]) and the temperature-corrected 6-31G** calculations have approximately the same rms % deviation from experiment, while the uncorrected 6-31G** results have the smallest rms % deviation from experiment of all theoretical treatments.

3.1.2

Crystal Densities: Ionic Molecular Crystals

In principle, the various methods used for crystal density prediction of neutral molecular crystals should be applicable to ionic systems. Indeed, group additivity schemes have been developed for ionic crystals [53, 54]. Unfortunately, the ionic partners that make up the formula unit in the ionic crystal introduce complications in implementing some of the other methods. The main challenge is properly defining the arrangement of the ionic partners

relative to one another. For several implementations of ab initio crystal prediction, the search algorithms cannot independently position or orient multiple ions that make up the formula unit during the generation of candidate crystals [32]. However, efforts are being made to extend this capability and initial results are promising [32, 55].

Attempting to energetically rank various arrangements of isolated ionic partners using quantum mechanical calculations might not be useful in all cases, since the most probable relative positions and orientations corresponding to the solid phase will be strongly influenced by the crystalline field, a property that cannot be captured in these calculations. Further, quantum mechanical geometry optimizations of isolated ionic partners can result in spontaneous reactions, e.g., proton transfer [56, 57]; the preservation of charge separation between the ionic partners in such a calculation is difficult to maintain.

However, quantum-mechanically calculated ionic volumes can be used to predict crystal densities of ionic crystals, where the ionic volume is defined to be that contained within a selected isosurface of electron density. Following Jenkins et al. [58], the volume of the formula unit M_pX_q of an ionic crystal is simply the sum of the volumes of the ions contained in the formula unit:

$$\text{Volume} = pV_+ + qV_- , \quad (3)$$

where M denotes the cation and X denotes the anion. This method of formula unit volume prediction was applied to 34 high-nitrogen ionic salts provided by Klapötke [35]. In this application, the ionic volume is assumed to be that contained within the 0.001 a.u. isosurface of electron density of the ion calculated at the B3LYP/6-31G** level. Two sets of ionic volumes were generated. The first set were calculated using molecular structures consistent with the experimental crystal and the second used equilibrium geometries resulting from a B3LYP/6-31G** geometry optimization. Unlike what we observed in our earlier application of this method to neutral CHNO molecular crystals, the formula unit volumes calculated using the experimental structures were in closer agreement with experimental values than those using the optimized structures. Upon examination of the optimized geometries of the cationic and anionic components of the ionic volumes, we found the following: for those ions that had no hydrogen atoms, the differences between the volumes of ions assuming the experimental structures with those using the optimized structures were very small (fractions of \AA^3). The largest differences were for ions that contained hydrogen atoms. Also, the magnitude of the difference in volume is directly proportional to the number of hydrogen atoms in the ion. This difference appears to be due to differences in the X – H (X = C, N) bond distances in the optimized and experimental structures. The B3LYP/6-31G** X – H bond distances are $\sim 0.1 \text{\AA}$ larger than those reported for the experimental structures.

In order to establish a correction factor to be used for calculations using optimized geometries of hydrogen-containing high-nitrogen ions, we first averaged experimental ionic volumes for each ion that is present in different ionic crystals. This averaged experimental ionic volume is then compared with the volume of the optimized ion. The difference between the averaged experimental and optimized ionic volumes scales almost linearly with the number of hydrogen atoms within the ion. This relationship allowed us to generate a correction factor for the high-nitrogen ionic crystals.

To calculate a “corrected” ionic volume using structures optimized at the B3LYP/6-31G** level, the formula is:

$$V(\text{corrected}) = V(\text{uncorrected}) - 0.976(\text{No. of Hydrogen Atoms in the ion}). \quad (4)$$

We did not attempt to define a thermal correction for these crystals. Calculated formula unit volumes using the experimental structures from the 34 high-nitrogen ionic crystals synthesized by *T. Klapötke* [35] had a rms deviation from experimental values of 4.6%. Formula unit volumes calculated using optimized geometries and corrected for the number of hydrogens had a 4.2% rms deviation from experimental values, whereas the uncorrected values had a 6.7% rms deviation from experiment. The rms deviation

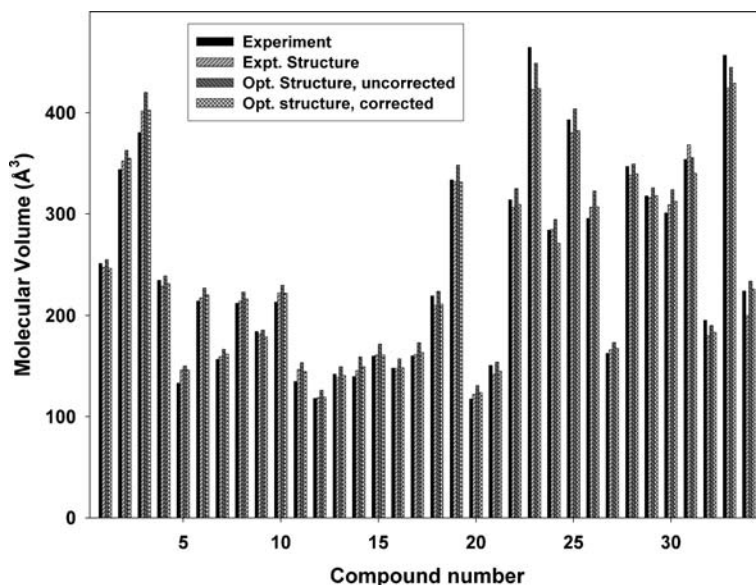


Fig. 2 Comparison of formula unit volumes of 34 high-nitrogen ionic crystals (*g/cc*) using experimental volume, predicted volumes using the experimental structures, predicted uncorrected volumes using optimized structures, and predicted volumes using optimized structures, corrected for the number of hydrogens (see text)

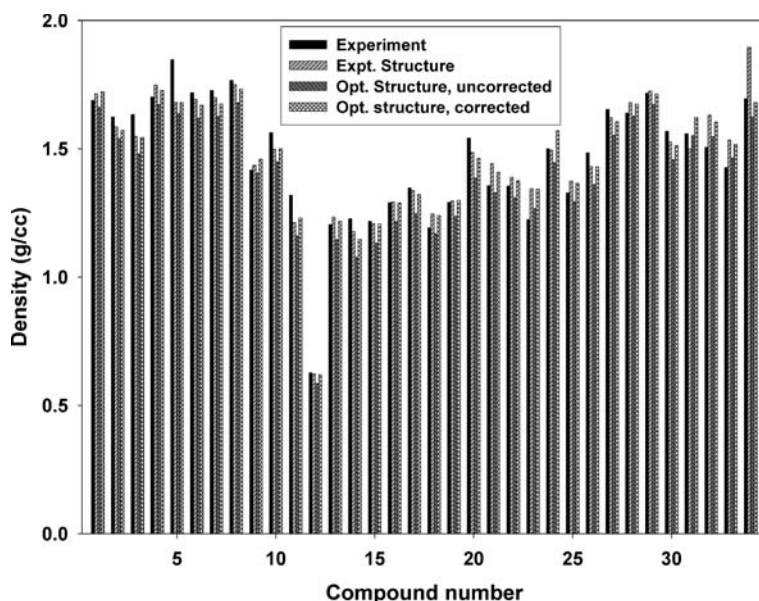


Fig. 3 Same as Fig. 2, except this provides a comparison of crystal densities

from experimental crystal densities using the volumes corresponding to the experimental structures is 4.7%, whereas the corresponding values using uncorrected and corrected formula unit volumes generated from optimized structures are 6.1 and 4.2%, respectively. Visual comparisons of the predicted and experimental molecules volumes and crystal densities are given in Figs. 2 and 3.

3.1.3

Solid Phase Heats of Formation: Neutrals

It can be argued that the solid phase heats of formation of a crystal can be calculated using highly accurate solid state quantum mechanical methods. However, computational obstacles rule out this approach. First, the only computationally feasible quantum mechanical approach to calculate the lattice energy of molecular crystals at this time is density functional theory. DFT does not adequately describe dispersion interactions, which are the main components of the binding energy in such crystals at ambient conditions [59, 60]. Secondly, this approach requires knowledge of the crystalline environment, and thus requires empirical information, which works against the overall goal to reduce dependence on such information through modeling. Solid phase heats of formation can be predicted using QSPR approaches [61–64], but their predictive capability might be limited to the chemical systems to which they were

parameterized. To our knowledge, there are no QSPR methods for predicting the solid phase heats of formation for high-nitrogen compounds.

The solid phase heats of formation of weakly bound molecular crystals can also be obtained using predictions of gas phase heats of formation and heats of sublimation through the following relation [65]:

$$\Delta H_{f(s)}^{\circ} = \Delta H_{f(g)}^{\circ} - \Delta H_{\text{sub}} \quad (5)$$

There are a variety of quantum-mechanically based methods to predict the gas phase heats of formation for neutral species. Politzer et al. have provided a detailed review of the various methods and their use in EM research [1], and we refer the interested reader to these. However, we will point out salient points from this review to illustrate applications of some of these methods to high-nitrogen compounds.

The numerous quantum-mechanically based schemes that exist for predicting the gas phase heats of formation include semi-empirical approaches that use atom or group equivalents. In this method, the gas phase heat of the formation is the difference in the energy of the molecule and empirically corrected energies of the molecule's component atoms or functional groups. The corrected energies, denoted as atom equivalent or group equivalent energies, are determined by fitting to experimentally measured values of heats of formation for representative systems. Several groups, including ours, have used this approach to develop a computational procedure for predicting the gas phase heats of formation of CHNO species [66–71]. Other more general methodologies that have a lesser degree of empiricism exist (e.g., the Gx methods [72]), although they require substantially more computational resources. As described by Politzer et al. [1], many of these methods predict gas phase heats of formation with a remarkable degree of accuracy. Calculations of heats of sublimation are almost exclusively performed using QSPR-like methods [66–68, 73–76]. The GIPF approach developed by Politzer for predicting this quantity has been particularly successful in applications to molecular crystals [66–71, 73–76]. Standard QSPRs using conventional molecular descriptors contained within commercial QSPR software [67] have also been developed for CHNO systems; however, these did not perform as well as the GIPF-based QSPRs when applied to a test set of molecules that were not included in the parameterization.

It cannot be assumed that any of the aforementioned computational methods that were parameterized using experimental information for CHNO systems would be transferable to high-nitrogen systems. In fact, application of the Byrd and Rice method [67] to a newly synthesized high-nitrogen compound (1-Methyl-5-(methylnitramino)-1*H*-tetrazole [4]) produced a solid phase heat of formation of 70.1 kcal/mol, far larger than the measured value (2.8 kcal/mol). Such a large discrepancy suggests that the method might not be transferable, and since there are so few (if any) data for gas phase heats of formation or heats of sublimation for high-nitrogen molecular crystals,

reparameterization of the equations used in Eq. 5 would be difficult. Thus, alternative approaches must be explored to treat high-nitrogen compounds.

The values for heats of sublimation of the CHNO crystals we surveyed typically ranged between 10–30 kcal/mol, with very few systems falling outside this range. Additionally, the heat of sublimation must always be a positive number. Conversely, the experimental gas phase heats of formation for the CHNO systems we have surveyed fall within a much larger range (from –70 to +100 kcal/mol [67]). In considering the disagreement of our approach to predicting solid phase heats of formation with the measured results for 1-Methyl-5-(methylnitramino)-1*H*-tetrazole, we concluded that the major source of the difference in our calculations and the measured value might be in the value of the gas phase heat of formation. We therefore undertook other quantum-mechanically based methods for predictions of the gas phase heat of formation of high-nitrogen compounds. In all calculations reported hereafter, the heats of sublimation used in Eq. 5 were calculated using the GIPF-methodology reported in [67].

The alternative methods used for predicting gas phase heats of formation are variants of the popular G3 methods [77] specifically the G3(MP2) [78] and G3(MP2)//B3LYP [79] approaches. The overall procedure involves multiple calculations at the HF/B3LYP, MP2, and QCISD(T) levels. The G3 method also attempts to correct for basis set size effects, zero point energy, and includes a general empirical correction. Therefore, like the atom/group equivalent approaches described above, this method includes some empiricism. However, G3 parameters are fitted to widely different chemical systems and a larger number of thermodynamic properties than those in our atom/group equivalent method [67, 68]. Additionally, the empiricism is not dependent on atom or group type, as are the atom/group-equivalent methods [1]. Further the G3 and atom/group-equivalent approaches use completely different methodologies for computing the energies. While the G3 and atom/group-equivalent approaches for predicting gas phase heats of formation rely on empirical fits, more accurate quantum mechanical approaches (such as CCSD(T) using a complete basis set) cannot be applied to any of the systems under consideration in this project (i.e., EMs) due to computational constraints. In fact, the G3(MP2) and G3(MP2)//B3LYP methods were developed to reduce computational cost compared to the original G3 [80] method at a small cost in accuracy. However, we found even these modified G3 calculations to be computationally infeasible for high-nitrogen systems larger than $C_{12}H_{14}N_8$. For this system, the G3(MP2) and G3(MP2)//B3LYP methods require excessive computational resources are not readily available outside of supercomputer clusters at this time.

The G3(MP2), G3(MP2)//B3LYP and our atom/group equivalent method were used to calculate the gas phase heats of formation of a set of neutral high nitrogen crystals; the values were added to the predicted heats of sublimation (using the GIPF method as described in Ref. [67]) to produce solid phase

heats of formation. The results and experimental values for the resulting solid phase heats of formation are shown in Fig. 4.

As evident in Fig. 4, the theoretical results are in reasonable agreement with each other for all compounds. Additionally, all calculated values are in agreement with the experiment except for Compound 2 (1-Methyl-5-(methylnitramino)-1*H*-tetrazole [4]). This suggests that either re-measurement of the heat of formation of Compound 2 should be performed or that there is some aspect of this system that is not captured by the quantum mechanical calculations. We emphasize that the two quantum mechanical approaches (atom/group equivalents versus G3 methods) for prediction of the gas phase heats of formation are sufficiently dissimilar that it is extremely unlikely that the error is within this portion of Eq. 1. There is a possibility, of course, that the heat of sublimation is poorly predicted for this system. That would not, however, explain the large discrepancy between the theoretical values and the measured result for Compound 2. Average and rms percent deviations were calculated using the seven other high-nitrogen compounds. Average percent deviations of the predictions from experiment are approximately the same for the group-equivalent and G3(MP2) approaches (these overestimate, on average, the experimental value by 5.3 and 5.6%, respectively). The average percent deviation of the G3(MP2)//B3LYP approach is

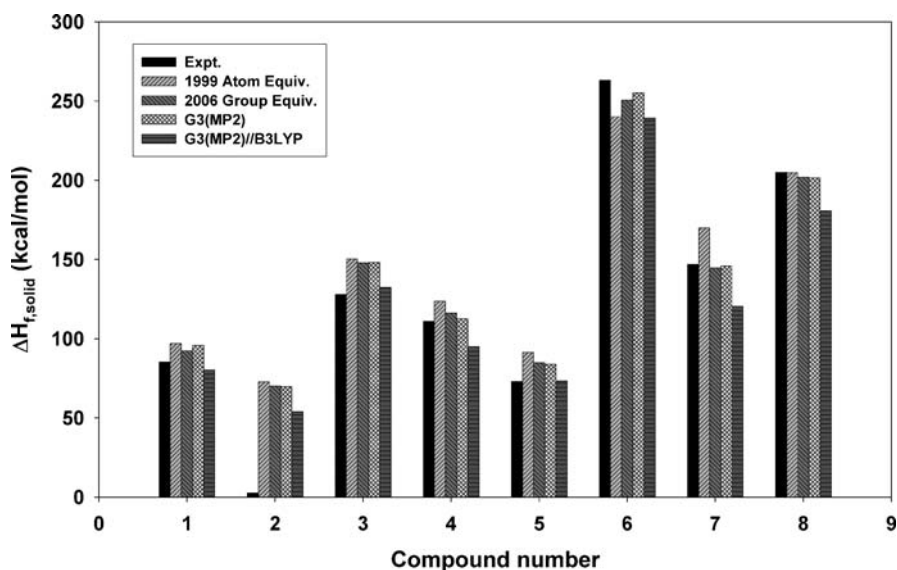


Fig. 4 Solid phase heats of formation for high-nitrogen crystals. Experimental values are taken from [4] and [223]. “1999 Atom Equiv” denotes calculations using the atom equivalent method described in [68]. “2006 Group Equiv” denotes calculations using the group equivalent method described in [67]. G3(MP2) and G3(MP2)//B3LYP denote calculations using variants of the G3 method [78, 79], respectively

larger (-7.9 kcal/mol) and underestimates the experimental value. The rms percent deviations from experiment are comparable for the group equivalent and G3 approaches, with the group equivalent and G3(MP2) having the best overall agreement with experiment (rms % deviation is $\sim 9.5\%$).

Of particular interest to us are the consistently close agreement between the group-equivalent method [67] and the G3(MP2) values. We remind the reader that the group-equivalent method was fitted to a smaller and more chemically specific set of experimental data (CHNO compounds with functional groups common to explosives) whereas the G3 parameters were fitted to a more general and substantially larger set of chemical compounds. Additionally, the group-equivalent approach requires considerably less computational resources. Since this good agreement between the two approaches has only been demonstrated for eight compounds, further investigation is required to determine whether this trend holds for a larger number of high-nitrogen compounds.

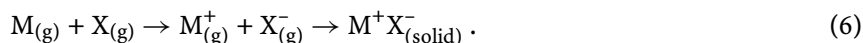
3.1.4

Solid Phase Heats of Formation: Ionic Crystals

As for the neutral crystals, we are not aware of any QSPRs developed to predict the solid phase heats of formation of high nitrogen salts, probably due to the relative scarcity of such experimental data required for establishing the correlations.

Since the crystalline binding energy in an ionic crystal is dominated by electrostatic interactions that are orders of magnitude larger than those in a neutral molecular crystal, the same scheme used for predicting the solid phase heat of formation for a neutral molecular crystal (Eq. 5) cannot be applied to ionics. Rather, the heat of formation of ionic compounds is determined using Born–Haber cycles [65] in which a series of reactions involving the ionic components are employed to produce the overall final result. Unfortunately, error is always introduced when quantum mechanical calculations are used in evaluating the reactions. Therefore, care must be taken in the choice of reactions used in the cycle.

The simplest of cycles might consist of three steps in which formation energies for each of the components can be calculated.



In this simple scheme, the first step requires the evaluation of the heats of formation of the neutral form of the charged components. The formation energies for the ionic components are then determined by evaluating the electron affinity or ionization energy and adding these to the heats of formation of the neutral moieties. The third step of the cycle requires the evaluation of the lattice enthalpy. Chemical reactions that generate the gas phase ionic components in Step 2 can also be used. Also, an alternative procedure for generating

the gas phase formation energies of the ions directly is presented by Beaucamp et al. [81]. In this work, gas phase heats of formation for the ions were determined using the method of atom equivalents. The atom equivalents were derived for a series of neutral compounds [82] and applied to five ammonium salts. These values and cohesive energies for these systems were used to generate solid phase heats of formation. The results are in reasonable agreement with the experiment, and further study on a larger number of high-nitrogen salts should be performed to determine the suitability of this method.

Unfortunately, there are limited (if any) experimental data that can be used to assess the quality of the calculations associated with each individual step in the aforementioned cycle. We are limited to comparing the overall final result with the experimental value of the heat of formation of the ionic crystal. This makes establishing the sources of errors in this cycle complicated.

It is possible to introduce significant error in the first step of this cycle. The magnitude of the error introduced in a quantum mechanical prediction of any reaction (including atomization) is dependent on the choice of reaction (i.e., the types and number of bonds that are broken or formed). The most accurate quantum mechanical approach for predicting the gas phase heat of formation of a new compound is to use isodesmic reactions [83]. This approach works very well if there are reliable heat of formation values for the products of the isodesmic reaction. If there is more than one possible reaction that will lead to the gas-phase ions in the cycle, it is possible that the quantum mechanical predictions will produce different results that are dependent on which reaction is chosen [84]. Also, generation of the gas-phase ions in Step 2 might require a sequence of reactions rather than a single reaction; this would introduce further error. Also, while there might be many different possible reactions leading to the charged moieties of interest, corresponding experimental data of the reaction products must be available. In lieu of that, Gx procedures [72] (or atom/group equivalent methods, if applicable to the system) can be used to predict the heats of formation of the various reaction products, but again, error is introduced.

To avoid the complications associated with identifying reaction sequences that can be used to produce gas phase formation energies of the ionic species, we will illustrate predictions of the solid phase heats of formation of a few high-nitrogen salts using the Born–Haber cycle given in Eq. 6. In this, gas phase heats of formation of the neutral forms of the charged species are first calculated (Step 1), and are followed by calculations of the electron affinity or ionization energy (Step 2) to generate the heats of formation of the charged moieties in the gas phase. The main drawback to this approach is the requirement that the neutral form of the charged species must be a minimum on the potential energy surface (PES). If it is not, then the Born–Haber cycle would require inclusion of reactions leading to the ionic moieties in Step 2.

We were encouraged by the good agreement between experimental and predicted values (using the G3 method) of gas phase heats of formation for

molecules contained in the eight high-nitrogen neutral crystals as described in the previous section. Therefore, we had a measure of confidence in using the G3 methods to predict gas phase formation energies of the neutral form of the charged species (Step 1). Unfortunately, there were many cases in which the optimized structure that is generated in the first step of the G3 calculations did not have the same chemical connectivity as that of the charged moiety in Step 2, indicating that the neutral form of the ion is not a minimum on the PES. The subsequent steps in the G3 calculations are all dependent on the molecular structure resulting from this optimization; therefore, it is essential that the molecular structure have the same chemical connectivity as that of the charged moiety. For the 26 ions corresponding to the various high-nitrogen salts provided to us by Klapötke [35], the most common result of a problematic geometry optimization was the dissociation of a hydrogen atom from the molecule. Since the geometry optimization performed in the first step of both of the two G3 approaches use a small basis set (6-31G*) and either the Hartree–Fock (HF) or B3LYP approach, it is possible that the problems are due to the application of an inadequate level of theory to treat these species. Tests of this hypothesis were performed by simply increasing the basis set size in the geometry optimization to include additional polarization and a diffuse function (6-31+G**). For all but four compounds a stable structure was found using B3LYP (we did not test HF). Applying the remainder of the G3(MP2) or G3(MP2)//B3LYP methodologies using these structures and the corresponding B3LYP/6-31+G** vibrational frequencies (scaled appropriately) produced gas phase formation energies. These revised G3 methods are denoted hereafter as modG3. The G3(MP2) and G3(MP2)//B3LYP empirical corrections will be applied accordingly, as modG3 has not been fitted for the correct empirical factor. Performances of the modG3 approaches were then evaluated through application to the original 8 neutral high-nitrogen compounds described in the previous section. The modG3 values track closely the G3 method from which the empirical correction is taken. For the G3(MP2) method, the average and maximum differences between the original and modified methods are 1.4 and 2.2 kcal/mol, respectively. For the G3(MP2)//B3LYP method, the average and maximum differences between the original and modified methods are 0.0 and 0.4 kcal/mol, respectively.

When determining the heats of formation of the ionic components beginning with the neutral forms of the species (Step 2), it is incorrect to use the vertical ionization energy, i.e., the energy required to add or subtract an electron without allowing structural relaxation upon ionization. In many of the cases we have examined, the neutral form of the ionic component has a substantially different structural conformation than that of the charged species; in such cases, the ionization energies or electron affinities must include the effects due to structural relaxation upon ionization. The energies resulting from such calculations will be referred to as “relaxed ionization energies”. Figure 5 provides a visual example of the structural relaxation upon ioniza-

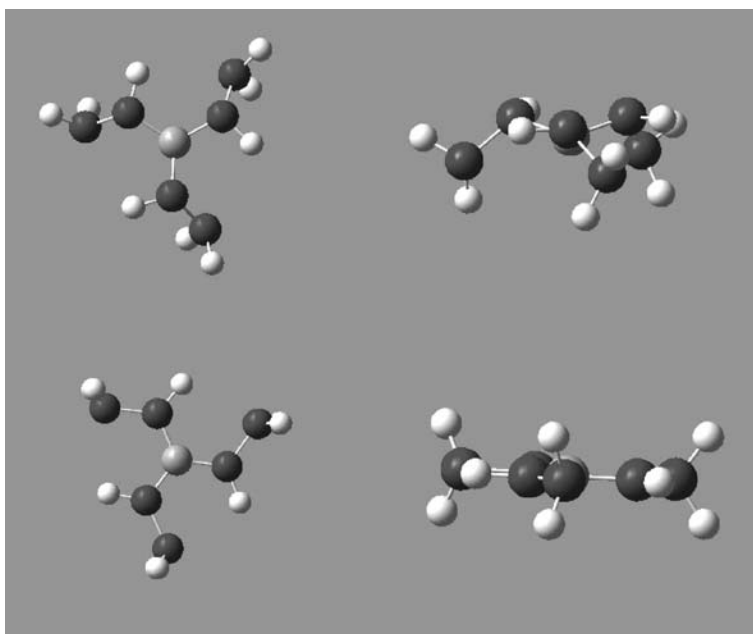


Fig. 5 Molecular structures of CH_9N_6 before (upper half of the figure) and after (lower half of the figure) ionization. Structures depicted in the left-most portion of the figure are top-down views of the moieties; structures in the right-most portions are side views of the moieties

tion for the CH_9N_6 moiety calculated at the B3LYP/6-31+G** level; it is clear that in some cases, structural relaxation would be a significant contributor to the final value of the ionization energy.

To determine the effect of structural relaxation on the ionization energy, we have calculated the relaxed and vertical ionization energies for the 20 high-nitrogen cations and 6 anions contained within various high-nitrogen salts synthesized by Klapötke [35]. The results are shown in Fig. 6. We found the effect to be particularly pronounced for the ionization energies; half of the compounds had structural relaxation energies on the order of 50 kcal/mol.

The final step in the evaluation of the Born–Haber cycle given in Eq. 6 is the determination of the lattice enthalpy, a measure of the energy required to dissociate the ionic crystal into its gaseous ions. The magnitude of this energy is quite large compared to the weaker intermolecular cohesive energies associated with organic molecular crystals (which are due mainly to van der Waals interactions), since it is a result of numerous long-range electrostatic interactions of ionic partners within the crystal. This value can be directly calculated by adding up all interatomic interactions within the crystal lattice if the positions of all atoms in the crystal are known and a reasonable description

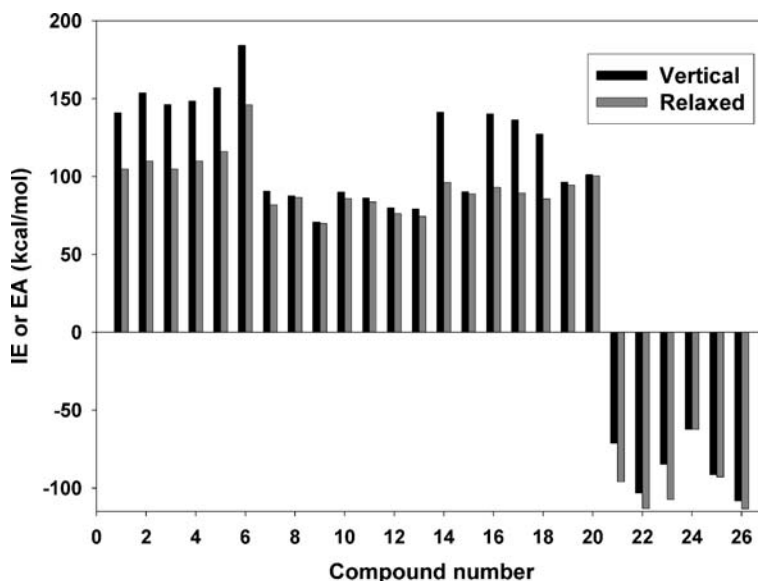


Fig. 6 Vertical and relaxed ionization energies for 20 cations and 6 anions used in high-nitrogen ionic crystals synthesized by Klapötke [35]

of the interatomic interactions is available (see, for example [58, 81, 85, 86]). Unfortunately, these two conditions cannot always be met. Therefore, numerous empirical schemes have been introduced to predict this quantity without knowledge of the crystal structure. One of the most widely used methods was developed by Kapustinskii, in which the lattice energy of a salt is estimated using values of the ionic radii [87]. Extensions to this approach have been made to better predict lattice energies of complex ionic crystals [88, 89]. Another method uses lattice energies calculated using point charges and experimentally crystallographic structures for a larger number of systems to generate a QSPR for cohesion energies in salts [85]. Politzer and Murray applied the GIPF approach to generate GIPF relations between lattice energies of ammonium, sodium and potassium cations with various anions [90]. A different QSPR-type method developed by Jenkins et al. has been applied to several high-nitrogen ionic crystals [58, 91]. This approach correlates the inverse cube root of the volume of the formula unit of an ionic crystal M_pX_q with its lattice potential energy $U_{\text{pot}}(M_pX_q)$. The lattice potential energy is related to the lattice enthalpy as follows:

$$\Delta H_L = U_{\text{pot}}(M_pX_q) + [p(n_M/2 - 2) + q(n_X/2 - 2)]RT, \quad (7)$$

where the values of n_M and n_X are dependent on whether the ions are monatomic, linear polyatomic, or non-linear polyatomic. Jenkins et al. [58, 91] parameterized the functional form for U_{pot} using lattice potential ener-

gies from [92]. These data consist of values derived from thermochemical cycles using experimental information and those from full scale calculations of the lattice potential energy of a crystal. In these calculations, crystal structural data (atomic positions) are specified, and an interatomic interaction potential (van der Waals terms plus Coulombic interactions, with partial charges assigned to nuclei) are used to produce the lattice energies. The information used in the parameterization was limited to salts containing alkali metal and alkaline earth cations (Li, Na, K, Rb, Cs, Mg, Ca, Sr, Ba). Goldschmidt radii of the cations (r_+) were used to define the cation volumes ($V_+ = 4/3\pi r_+^3$). Anion volumes were determined first by calculating the molecular volume of the alkaline earth/alkali metal salts (using experimental values, $V_{\text{unit cell}}/N_{\text{unit}}$) and subtracting the volumes of the cations.

A possible source of error associated with this approach might be due to the variable reliability of the fitting data [92]. Another source of error associated with this approach when applied to high-nitrogen salts is the types of salts used in the parameterization. In this parameterization of the QSPR, the cations of the salts were limited to alkaline metal or alkaline earth atoms (small and spherical volumes). The anion volumes were derived from experimental information about the salts and the values assigned to the alkali metal or alkaline earth cations. It is not known whether this method is transferable to salts that have significantly different chemical compositions, and for which the cations are substantially different in shape and size (such as some of the new high-nitrogen salts).

A rough assessment of the Jenkins approach for predicting lattice energy for high-nitrogen salts can be performed through direct calculations assuming the experimental structure and reasonable interaction potentials (such as that developed by Ammon, described earlier). At this time, we have not attempted nor are we aware of such an assessment. We will, however, use the Jenkins approach for purposes of illustrating prediction of the heat of formation of ionic crystals, specifically, three recently synthesized high-nitrogen salts [10]. These are presented and compared with experimental and other theoretical predictions in Table 2. The theoretical result generated by Gálvez-Ruiz et al. [10] invoked a Born-Haber cycle using reactions along with proton affinities, whereas we utilize the procedure outlined above. Additionally, the

Table 2 Heats of formation of tetrazolium salts

Species	ΔH_f , MX(s) (kcal/mol)		
	Expt. [10]	G2 [10]	modG3(MP2)
1-5-Diamino-4-methyl-tetrazolium nitrate	8.4	41.7	47.5
1-5-Diamino-4-methyl-tetrazolium azide	138.1	161.6	165.4
1-5-Diamino-4-methyl-tetrazolium dinitramide	45.3	92.1	94.9

Gálvez–Ruiz et al. calculations used the G2 method [93], which has different empirical corrections and approaches than the G3 methods we used. Note that the two theoretical approaches, which would have distinctly different sources of error, are very close in value for the three compounds. They both, however, overshoot the experimental values by 30–40 kcal/mol. Since the common element between the two theoretical methods is the Jenkins approach [58, 91] for predicting lattice energies, it is possible that the major discrepancy between experiment and theory is within this step. However, before this conclusion can be made, the Jenkins method should be evaluated as suggested above.

3.2

Prediction of Vulnerability and Environmental Hazard

The performance potential of a new EM is not the only factor considered when determining whether to pursue synthesis or full-scale development. Of equal concern are the environmental impact of the material and its vulnerability to accidental initiation. Unfortunately, both categories of potential hazard encompass wide ranging phenomena. Environmental hazards include effects of the material on aquatic and mammalian life, ground water and atmospheric fate and transport, human toxicity or carcinogenicity. Vulnerability of an EM refers to different ways in which accidental initiation can occur, including electrostatic discharge, friction, shock, or impact, the results of which differ depending on the type of initiation. Both types of hazard represent diverse sets of extremely complex and interrelated physical-chemical properties and phenomena that have not been extricated or identified. Consequently, little progress has been made in developing a fundamental, detailed characterization of either type of hazard. Rather, most efforts have been directed to developing QSAR/QSPRs to predict potential hazards. This approach has been used to a small extent for predicting environmental hazards of conventional EM due to limited empirical information [94–101]. To our knowledge, there have been no published reports of predictions of environmental hazards of high-nitrogen EMs.

There exists a large body of empirical vulnerability data for conventional EM for which numerous researchers have correlated molecular or material properties [102–156]. Of these, a large number of the molecular properties used in the correlations were predicted using semi-empirical or quantum mechanical methods. While many of these are quite useful in identifying potential vulnerability of an EM, they should not be used to justify mechanistic arguments [157, 158]. Additionally, as with all QSPR approaches, the predictive capability is strongly dependent on the quality of the empirical information used in the parameterization. Unreliable empirical information used in the parameterization could result in a highly inaccurate tool. For vulnerability, the majority of the empirical data consists of results of drop-

weight impact tests, a crude and rapid method used to qualitatively assess the sensitivity of a material to impact. This test is notoriously inaccurate and its results are strongly dependent on the conditions under which the experiments are performed. Therefore, correlations made with the results could incorporate flawed measurements. Further, it is well established that the sensitivity of a material to accidental initiation is influenced by material morphology, something that cannot be captured with such simple correlations. Finally, there is never a guarantee that a QSPR developed for one series of compounds is transferable to a different chemical family. Since several correlations developed for conventional CHNO explosives are not transferable across chemical families, it is not expected that such correlations would be maintained for high-nitrogen HEDMs. We note, however, that two studies [5, 6] applied a QSPR-type method to assess impact sensitivity using quantum mechanically calculated electrostatic potentials [102, 159] to several high-nitrogen solids and showed that the correlations were maintained. However, since these methods were developed for CHNO explosives, similar applications to a larger number of high-nitrogen systems must be performed before it is concluded that such a correlation is indicative of sensitivity to impact for these systems. Clearly, advances in development of predictive methodologies in this area are needed.

4

Novel Polynitrogen Species

The earlier portions of this chapter have focused on computational methods of high-nitrogen compounds that are produced using conventional concepts of inorganic and organic chemical synthesis and known functionality [160]. This portion of the chapter will examine recent efforts to predict exotic forms of all-nitrogen molecules using quantum mechanical theories. Earlier predictions have been described in previous reviews of such compounds [161–163] and will not be repeated here. Since then, many larger all-nitrogen compounds in a variety of cyclic, acyclic or caged conformations have been explored using theoretical chemistry. The species investigated include ionic clusters [164–166], cylinders [167], cages [168–176], nanoneedles and nanotubes [177] and helices [178]. Isomers of smaller systems (N_7 [179], N_{10} [180] and N_{12} [181]) have also recently been reported. While the majority of these studies have focused on the evaluation of these novel forms of molecular nitrogen, at least one study uses theory to provide guidance in developing synthesis routes for an all-nitrogen system [182].

As shown in the earlier studies on smaller systems [161–163], stability of these compounds is perhaps the overriding issue that must be addressed. Thus, all of these calculations have several common goals: To establish a) whether the structure is a local minimum on the potential energy surface

(PES); b) its degree of stability with respect to unimolecular decomposition; and c) the structural features that stabilize the species. A successful demonstration of the ability of theory to predict stability of such compounds is given by Dixon et al. [183], in which high-level quantum mechanical calculations [CCSD(T)] indicated that $N_5^+N_3^-$ and $N_5^+N_5^-$ salts are not stable; these results were subsequently confirmed by experiment. Theory has also been used to computationally engineer structures to enhance stability through the addition of non-nitrogen atoms [184–191]. All of these studies have the potential to aid in the selection of the most promising all nitrogen molecular system for synthesis. The only caveat is that in most of these studies, only modest levels of quantum mechanical theory (mainly DFT and MP2) have been applied due to the system sizes, thus precluding the application of more accurate quantum mechanical methods. DFT and MP2 methods are adequate to identify local minima on the PES and provide estimates of stability to unimolecular decomposition. However, the extreme complexity of the electronic structure of these exotic forms of nitrogen requires higher levels of QM theory in order to quantify the degree of stability. This is illustrated by recent conflicting theoretical calculations on N_7 clusters using DFT and MP2 and a variety of basis sets [179, 192]. Using the G3 method, Wang et al. [192] predicted that the most stable of N_7 conformers is an N_5 ring with an N_2 side chain, but Zhao et al. found that the stability of the conformer was dependent on level of theory and basis set [179]. For such a case, only a higher level quantum mechanical treatment could resolve the discrepancies. It is unfortunate that at this time, the sizes of systems being explored exceed the computational bounds required for the necessary high-level treatments. But as history has shown, advances in computational power will allow for increasingly larger systems to be investigated using more accurate quantum mechanical treatments.

5

Novel High Pressure Phases of Nitrogen

Interest in high and all-nitrogen materials is not exclusive to the energetic materials community; the high-pressure physics community has been searching for novel, high-pressure forms of nitrogen for years [193–203]. As for all molecular systems, it is presumed that sufficient application of pressure will lead to the destruction of covalent bonds. For nitrogen, whose triple bond introduces extra complexity over singly bonded molecular solids, it is expected that any pressure-induced transformation will proceed first through formation of an intermediate polymeric network of singly or doubly bonded atoms, similar to that of other group V elements (phosphorus and arsenic) before losing covalency completely at higher pressures. Thus, experimental verification of such high-pressure non-molecular phases of nitrogen has long been

sought, but it has only been recently that such was achieved [199–203]. In addition to these non-molecular phases of nitrogen, several molecular phases over wide temperature and pressure ranges have been experimentally determined [193–198, 204, 205].

Theoretical studies, on the other hand, have predicted a variety of non-molecular structures at pressures for which only molecular phases have been observed. These include a monatomic simple-cubic phase [206–208], a semi-metallic arsenic structure A7 [206], a metallic, simple-tetragonal phase [206, 209], and the cubic gauche (CG) structure [205, 207, 210–213], for which recent experimental evidence has been given [203]. Results from theoretical calculations also predict other polymeric forms of nitrogen, as will be described hereafter.

The disparity between the theoretical predictions and experimental verifications can be attributed to several factors, including large energy barriers that might inhibit any transition leading to the polymeric forms upon compression of the molecular crystals. These can be explored using theoretical methods, as will be shown here. This section will describe detailed, *ab initio* descriptions of the electronic structure of high-pressure phases of nitrogen, and *ab initio* quantum molecular dynamics (QMD) calculations, in which integration of the classical equations of motion using quantum mechanical forces produce time-dependent atomic positions and velocities. The latter calculations have been used to identify stable structures through quenching of materials simulated at high temperatures and pressures. QMD calculations are also used to establish ranges of metastability. This section will be limited to discussions of quantum mechanical calculations, with a focus on density functional theory treatments of these systems, and will not include discussions of classical molecular simulations of high-pressure phases of molecular nitrogen.

It was generally assumed that pressure-induced transformation of molecular nitrogen would progress first to a chain-like structure, then to a layered structure and finally to a bulk, or extended solid, structure. Early theoretical work, therefore, focused on establishing the simple chain, layered, and bulk structures known from other Group V elements, including A7 [206], and black phosphorus (BP) [207]. Early calculations of the various forms of non-molecular nitrogen predicted that the layered A7 and BP structures are lower in energy than the chain and bulk structures [206]. Later calculations predicted that the transition from molecular nitrogen would progress directly to the bulk CG structure, which is unique to nitrogen, bypassing formation of layered and chain structures [207, 210–213]. The CG form of nitrogen is a fully coordinated three-dimension structure, and is an analog to the diamond structure of carbon. Calculations predict it to be substantially lower in energy than the other non-molecular phases A7 and BP. Another chain structure was recently predicted that is energetically competitive with CG and will be detailed hereafter.

The majority of the early calculations in which new structures of nitrogen were identified resulted from deformations of a simple cubic lattice of nitrogen. One of us pursued a series of DFT studies to identify structures resulting from compression of the highest pressure known phase of nitrogen, the non-cubic molecular ϵ phase [214]. These results will be presented here. Some of these calculations were performed for systems that had been previously identified through other theoretical calculations using a lower level of quantum mechanical theory [207]. These calculations were redone at the higher level [using the generalized gradient approximation (GGA)] to verify relative energies.

We first confirmed the CG form (Fig. 7), and also found that CG can exist in either a left or right-handed form. These two forms are degenerate in energy and suggest that equilibration to one form or the other might be difficult. Instead, these features on the potential energy surface suggest that an amorphous mix of these two forms might result upon compression.

Although Barbee [211] has shown the CG structure to be stable at low temperature and zero pressure, we performed QMD simulations for various temperatures and pressures ranging from 0 and 50 GPa to test for instability. NVE simulations with an initial temperature of 300 K and a volume consistent with the low-pressure form of CG resulted in the dissociation of the structure into molecular nitrogen and a large energy release. The same result was observed for an NVE simulation with an initial temperature of 400 K and a volume corresponding to 50 GPa at 0 K. When these structures destabilized, the transition was extremely rapid and the temperature increased to over 10 000 Kelvin in a few time steps.

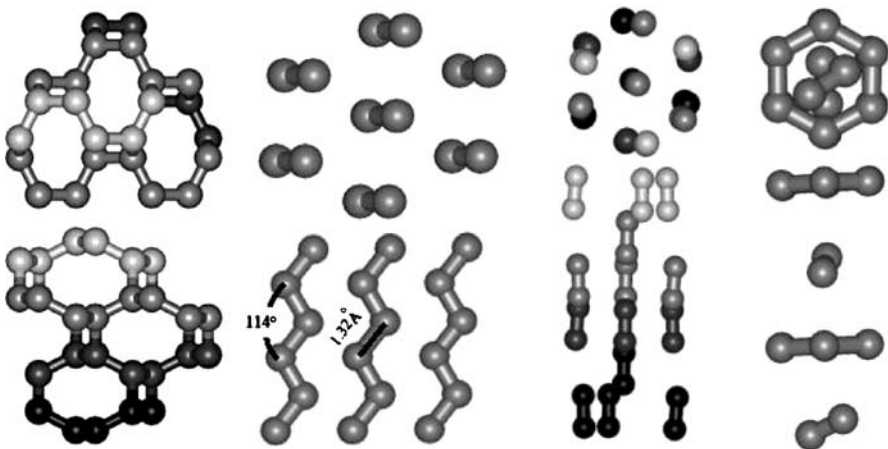


Fig. 7 Diagrams of various forms of compressed nitrogen. The structures are, from *left to right*, cubic gauche (CG), the hexagonally packed chain (HPC), ϵ -nitrogen, and Hexagonal N6 rings

Calculations performed by us and others produced an assortment of chain structures [207, 210, 212, 213], all but one of which are not energetically competitive with CG. The only energetically competitive chain structure was found in DFT optimizations of a forty-eight atom cell initially arranged in the high pressure molecular ε phase of nitrogen. Minimization of this cell at 220 GPa produced a series of hexagonally packed chains (HPC). At pressures above 400 GPa, this structure transforms into a fully connected structure with each atom being bonded to three others. With only a small increase in energy, this chain structure can be idealized as a deformed simple hexagonal lattice and a two-atom basis. The chains zig-zags, with the major axis of the chain parallel with the c -axis. The minor axes of all the chains are parallel to each other and perpendicular to one of the hexagonal lattice vectors. The idealized unit cell with a simple hexagonal lattice is given by the lattice vectors: $(a, 0, 0)$, $(a/2, \sqrt{3}a/2, 0)$, $(0, 0, c)$; the Cartesian atomic coordinates: $\pm(0, b, c/4)$, where $b = \sqrt{d^2 - c^2}/4$, and d is the bond length of 1.32 Å, and the a/c ratio is 0.9 with a lattice constant of 2.555 Å. The chains have bond angles of about 114° at low pressure. The HPC structure is shown in Fig. 7.

Two tests of stability were performed for this phase at pressures near ambient. For the first test, each atom in a sixty-four atom cell was randomly displaced by a maximum of 1% of the bond length in each Cartesian direction. A subsequent geometry optimization was performed, with a target pressure near that of the initial structure (~ 100 bar) in which atoms were not displaced. The system converged to the undisturbed state. This test was repeated, except all of the atoms were displaced by 5% of the bond lengths; the results did not change. For the second test, atoms were displaced along the line connecting atom pairs within the chain. This test was designed to facilitate transformation to a molecular nitrogen phase. Alternating bonds in the chain were contracted by 2% (resulting in an approximate two-percent expansion of the remaining bonds), after which a geometry optimization was performed. The system again converged to the undisturbed state. The same test was repeated except the bonds were contracted or expanded by 10%. The energies of the states in which the atoms are randomly displaced or displaced along bonds were higher than the HPC state by as much as 0.6 eV/atom. This indicates that there are substantial barriers to transition along these two paths. The HPC chain structure is distinguished from the other chain structures we investigated since it is energetically competitive with the CG phase, whereas the other chain structures were substantially higher in energy. The rapid increase in energy upon perturbation of atoms within the HPC from the equilibrium position and the higher energy of very similar chains suggest that the specific packing in the HPC phase is the basis for its low energy and stability. It is interesting that theoretical predictions of all-nitrogen molecules include molecular structures that resemble the hexagonally packed chains [163]. In these structures, the intramolecular bond lengths and angles

are very similar to those of the chain. It is conceivable that such molecules could be packed into the crystalline state, perhaps at near ambient conditions.

Figure 8 shows the energy curves for the HPC and CG structures. The energy for the chain structure is slightly lower than CG at pressures well above the transition pressure (i.e., $V < 5 \text{ \AA}^3$), but is approximately the same or slightly higher than CG for the pressure range near the transition pressure. The difference in the energies of these structures is within the error of the GGA approximations, making the HPC structure practically degenerate in energy with the CG structure between approximately 5 and 6.5 \AA^3 . At pressures less than the transition pressure the HPC is lower in energy than CG.

In the HPC phase, each atom has valence electrons symmetrically bonded to two other atoms. For such a case, it is expected that the bands at the Fermi energy would be π -bands, similar to those in graphite. However, the nearly one-dimensional nature of the HPC chain structure should lead to a large, metallic, nearly flat Fermi surface unlike the semi-metallic Fermi surface in graphite. Indeed, the chain structure is metallic in nature as evidenced by the band structure in Fig. 9. The band structure of an identical single isolated chain is provided for comparison. Only the bands along the major axis of the chain are shown, as directions normal to the major axis are uninteresting, as expected for chains. We explored the possibility of a Peierls distortion leading to an insulator [215], but this is not found in the tests on distorted structures

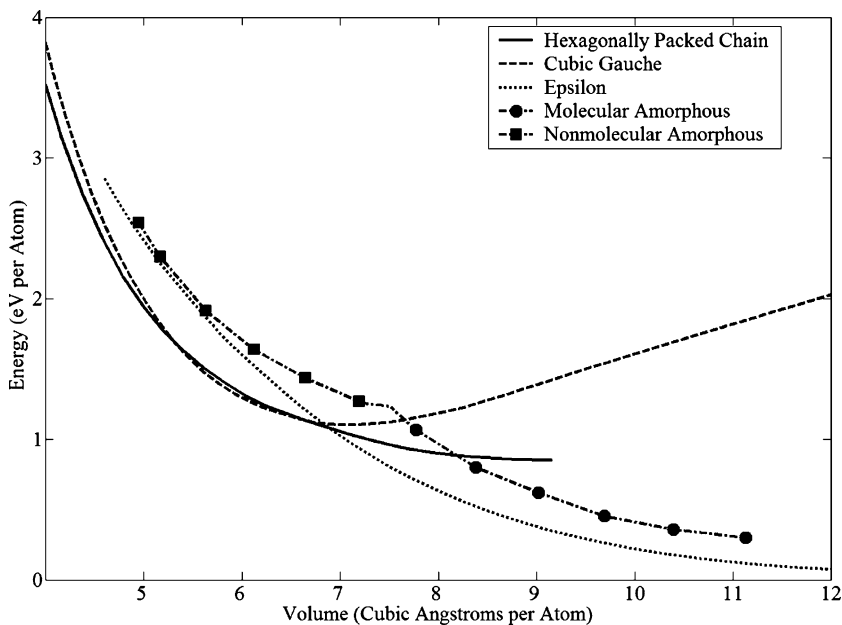


Fig. 8 Energy versus volume curves for the HPC, CG, ϵ , amorphous molecular and amorphous nonmolecular phases of nitrogen

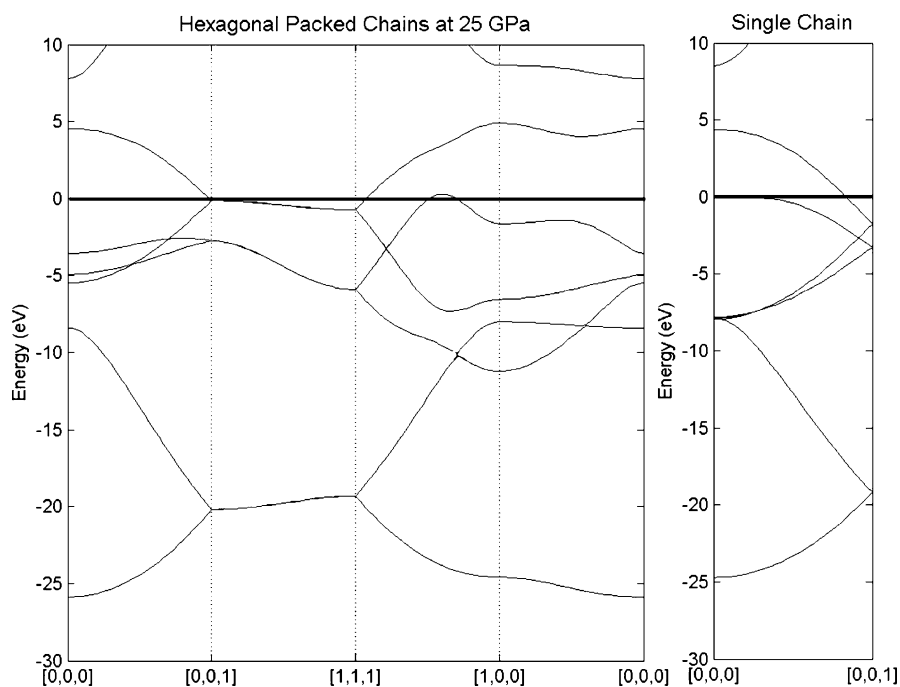


Fig. 9 Band structure of the HPC structure (*left-hand side*) and a single isolated chain (*right-hand side*). The Fermi energy is represented by the *solid dark line*

reported above. Presumably the stability of the metallic nature of the HPC phase is due to the fact that the system is not truly one-dimensional.

A metallic form of nitrogen is of great interest because of the possibility of superconductivity at a high transition temperature in such a phase. This possibility is suggested both by the small mass and by the large valence of nitrogen. Indeed, one of the highest temperature elemental superconductors known is sulfur at high pressure [216–218], first predicted by theory [219]. The small mass of nitrogen implies a large Debye temperature, and the large number of valence electrons of nitrogen implies a large carrier density in a metallic phase. Both of these properties will tend to enhance the transition temperature. The electron–phonon interactions should be large for this element, as for other first row elements. On the one hand, the electron–phonon interaction is responsible for the instability of structures like the simple cubic; on the other hand, if the stable structure is metallic, then the electron–phonon interaction could lead to a high superconducting transition temperature T_c . Thus nitrogen can be an example of the competition between high T_c and structural instabilities [206]. Such a question invites further study.

An interesting molecular phase that was identified during the exploration of the conformational space of nitrogen was that of hexagonal N_6 , shown

on the right side of Fig. 7. While this is a molecular phase, it is not a diatomic molecular phase, and thus has the potential for large energy release upon transition to the lower-energy diatomic molecular phase. When the ε structure is minimized at ~ 60 GPa, this non-diatomic molecular phase appears. The ε structure transitions into a hexagonal-close-packed structure that consists of a unit cell containing one N_6 and one N_2 molecule, with the N_2 molecule centered coaxially between the N_6 molecules on alternating levels. The transition to this phase creates hexagonal N_6 from the disk-like molecules forming columns. The sphere-like molecules remain molecular and are centered between two coaxial N_6 molecules. These columns of N_6 are packed hexagonally, with adjacent columns offset along the axis of the column by a third the distance between N_6 in the column. This offset alternates direction going clockwise for each of the six neighboring columns. This structure has an energy that is equivalent to the molecular ε structure at the same volume and is a local energy minimum between 18 and 145 GPa. Since this is a relatively high-energy structure, no further stability testing was performed. At the lower end of the pressure range, the hexagonal structure transforms back into the ε molecular structure. Interestingly, as the pressure on this structure is increased beyond 145 GPa, the N_6 molecules begin to bond to each other at adjacent corners of the hexagons, forming a three dimensional structure not entirely dissimilar to the cubic gauche structure while maintaining the encapsulated N_2 molecules. While the energy of this structure is clearly above the other structures shown, it may still be physically observable if the transition barriers are large enough. It may be possible to obtain this phase by heating then cooling the ε phase at pressures below 100 GPa. Thus, this structure may be a candidate for the θ phase [202]. In addition, N_6 rings have been observed by Vogler et al. [220].

A second series of calculations were performed that were different in spirit than those described heretofore, in which the ε -form of molecular nitrogen was compressed to generate new structures. In this series, atomic nitrogen gas at high temperature and pressure was rapidly cooled at constant pressure. These calculations used QMD to produce the quench. The quenches of the hot atomic nitrogen gas produced, as expected, amorphous final states, but the final pressure at the end of the quench determined whether the final state would be molecular or a connected network of nitrogen. The molecular phase was only found below 100 GPa. At 100 GPa and above, the quenched configurations were interconnected networks, some of these would have a few diatomic nitrogen molecules, but all other nitrogen atoms are connected by a path of bonds to the other atom in the structure. The transition pressure of 100 GPa agrees well with that obtained from analysis of experimental results [200] (~ 100 GPa). In addition Raman studies of nitrogen have found evidence for the nitrogen diatomic bond destabilization at about 100 GPa [197, 220].

One of our major findings is that quenches to higher pressures yield amorphous networks of singly, doubly and triply connected atoms. The number of singly connected atoms is small, but the ratio of doubly to triply connected atoms is close to one. This may be interpreted in one of two ways, one being that the doubly connected atoms are either stacking faults or an artifact of the unphysical nature of the quench, but not energetically favored. Alternatively, and in light of the predictions of the HPC chain, these doubly connected atoms may actually be small examples of such chains and thus energetically competitive with the triply bonded form.

A typical amorphous structure is shown in Fig. 10. Bonds that cross the periodic boundary are not shown, thus giving the appearance of more singly and doubly connected atoms than are in the structure. For the structure represented in Fig. 10, there are eight singly connected atoms, twenty-eight doubly connected atoms, and twenty-eight triply connected atoms. All of the nitrogen networks produced in our simulations had several common characteristics. First, all atoms are bonded to one, two, or three other atoms. The number of singly bonded atoms ranged from four to ten, but the number of atoms bonded to two atoms or to three atoms was the same in each of the networks tested (~ 27 – 30). Secondly, the dihedral angles for pairs of triply connected atoms in the amorphous structure were similar to those in the CG structure. Thirdly, the amorphous networks transition to a liquid with increasing temperature. The atoms do not move freely, but bonded pairs will swap neighbors.

To test the stability of the amorphous networks, the pressure on the simulation cell was slowly released until the structure began to break apart. Even

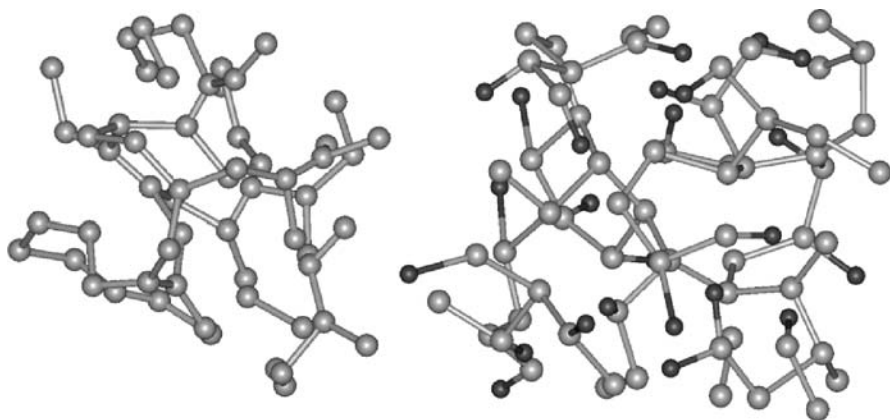


Fig. 10 *Left-hand side:* A typical amorphous structure, quenched to 200 GPa. The bonds that cross the periodic boundaries are not shown. *Right-hand side:* Passivated amorphous nitrogen structure. The hydrogen atoms are shown in *dark gray* and the nitrogen in *light gray*

at low temperature the amorphous structure became unstable between 80 and 100 GPa, the same pressure range where the quenches of the hot reactive nitrogen switched from producing molecular to non-molecular structures. For the amorphous configurations, the transition from the non-molecular to molecular phase begins with a dangling nitrogen atom breaking away with its single nearest neighbor forming a diatomic molecule. In all cases we observed, this dangling nitrogen was bound to only one other atom. We concluded that these singly bonded, dangling nitrogen atoms are the seeds of instability in the amorphous structure. The formation of the diatomic molecule completely destabilizes the system and the transformation from the polymeric phase proceeds rapidly. At higher temperatures the transformation occurs in the same pressure range, indicating that it is not a temperature-driven transition. The transition pressure of the quenches and the back transition pressure agree with the experimentally predicted equilibrium transition pressure of 100 GPa [201].

We were able to stabilize the amorphous network at pressures greater than 80 GPa by passivating all singly connected atoms. A passivated structure (Fig. 10) was constructed from an amorphous structure (used in the stability tests) by adding hydrogen atoms in the following manner. For a singly connected nitrogen (denoted N'), two hydrogen atoms were added such that all $X - N' - X$ angles are 120° , ($X = N, H$). The $X - N'$ bond lengths were set to 1 Å. Doubly connected nitrogen atoms had a single hydrogen atom added so that both $H - N - N$ angles are the same and are obtuse. Therefore, the passivated structure is one in which all nitrogen atoms are bonded to three other atoms. The coordination of this structure is consistent with the experimental material, which estimates a coordination of 2.5 at pressures of 180 GPa [199]. This passivated amorphous nitrogen structure was minimized with respect to energy at constant pressure. The stability of the passivated amorphous structure was examined in the same way as the amorphous structure. The passivated structure became unstable between 60 and 80 GPa irrespective of the temperature of the simulation. These theoretical studies clearly demonstrate that passivating the amorphous structure with hydrogen has a stabilizing effect; experiments are currently being performed to explore these ideas [221].

Given the number of energetically competing structures and the experimentally implied large barrier to transition, formation of an amorphous structure upon compression of nitrogen is not surprising. However, new crystallographic data [222] show that there might be some regularity to the experimental structure. Upon examination of the amorphous structures produced by the quench, we find evidence of both the cubic gauche and chain structures. The triply connected atoms have dihedral angles that are consistent with cubic gauche structure. The doubly connected atoms are chain-like. The fact that they occur with roughly equal probability in the amorphous structures implies that neither is strongly favored over the other and thus,

this amorphous phase might contain an equimolar mixture of such doubly and triply connected atoms. NVT QMD simulations of the amorphous liquid did not produce a change in the number of bonds an individual atom has but shows that bonded atoms swap neighbors. This suggests that transforming between doubly and triply connected bonding may be energetically improbable. These theoretical results suggest that the observed experimental structure could be composed of an amorphous collection of small clusters of the different competing structures.

Although the results described in this section have not completely elucidated all of the complexities associated with pressure-induced structural phase transitions of nitrogen, the calculations have demonstrated how carefully designed theoretical simulations can be used to predict novel and interesting high pressure phases of nitrogen.

6

Concluding Remarks

The design and synthesis of novel high-energy, high-nitrogen materials is of great importance in advancing the field of energetic materials. Developments in computational chemistry and physics-based modeling such as those described herein are crucial in producing rapid breakthroughs in the development of these new materials. Computational exploration of notional materials allows for screening among potential candidates, assessing possible synthesis routes, or identifying conditions under which the materials exist. This, in turn, leads to a substantial reduction of time, money and waste streams associated with synthesis and testing of inferior materials or exploring materials under inappropriate experimental conditions. While progress is being made to develop accurate computational tools that are applicable to this emerging class of EMs, there are still significant challenges to overcome, particularly in the development of methods to assess environmental and vulnerability hazard. However, the potentially large cost and time savings compel further investment in developing theoretical procedures to complement experimentation leading to the synthesis and design of these new materials.

References

1. Politzer P, Murray JS (eds) (2003) *Energetic Materials: Part 1. Decomposition, Crystal and Molecular Properties (Theoretical and Computational Chemistry)*. Elsevier Science, Amsterdam
2. Politzer P, Murray JS (eds) (2003) *Energetic Materials: Part 2. Detonation, Combustion (Theoretical and Computational Chemistry)*. Elsevier Science, Amsterdam
3. Drake GW, Hawkins TW, Boatz J, Hall L, Ashwani V (2005) *Propellants, Explos, Pyrotech* 30:156

4. Karaghiosoff K, Klapötke TM, Mayer P, Piotrowski H, Polborn K, Willer RL, Weigand JJ (2006) *J Org Chem* 71:1295
5. Klapötke TM, Mayer P, Schulz A, Weigand JJ (2004) *Propellants, Explos, Pyrotech* 29:325
6. Hammerl A, Klapötke TM, Mayer P, Weigand JJ, Holl G (2005) *Propellants, Explos, Pyrotech* 30:17
7. Klapötke TM, Karaghiosoff K, Mayer P, Penger A, Welch JM (2006) *Propellants, Explos, Pyrotech* 31:188
8. Klapötke TM, Mayer P, Schulz A, Weigand JJ (2005) *J Am Chem Soc* 127:2032
9. Hammerl A, Klapötke TM, Nöth H, Warchhold M (2001) *Inorg Chem* 40:3570
10. Gálvez-Ruiz JC, Holl G, Karaghiosoff K, Klapötke TM, Löhnwitz K, Mayer P, Nöth H, Polborn K, Rohbogner CJ, Suter M, Weigand JJ (2005) *Inorg Chem* 44:4237
11. Geith J, Klapötke TM, Weigand J, Holl G (2004) *Propellants, Explos, Pyrotech* 29:3
12. Hammerl A, Klapötke TM, Nöth H, Warchhold M, Holl G (2003) *Propellants, Explos, Pyrotech* 28:165
13. Hammerl A, Klapötke TM (2002) *Inorg Chem* 41:906
14. Alavi S, Thompson DL (2005) *J Phys Chem B* 109:18127
15. Cadena C, Maginn EJ (2006) *J Phys Chem B* 110:18026
16. Strachan A, van Duin ACT, Chakraborty D, Dasgupta S, Goddard III WA (2003) *Phys Rev Lett* 91:098301
17. Boyd S, Gravelle M, Politzer P (2006) *J Chem Phys* 124:104508
18. Smith GD, Bharadwaj RK (1999) *J Phys Chem B* 103:3570
19. Sorescu DC, Rice BM, Thompson DL (1997) *J Phys Chem B* 101:798
20. Todeschini R, Consonni V (2000) *Handbook of Molecular Descriptors*. In: Mannhold R, Kubinyi H, Timmerman H (eds) *Series of Methods and Principles of Medicinal Chemistry*, Vol. 11. Wiley, New York, p 667
21. Karelson M, Lobanov V, Katritzky AR (1996) *Chem Rev* 96:1027
22. Bartlett RJ (2003) *Electron Correlation from Molecules to Materials*. In: Gonis T, Kioussis N, Ciftan M (eds) *Electron Correlations and Materials Properties 2*. Kluwer Academic/Plenum Publishers, New York, p 219
23. Helgaker T, Jorgensen P, Olsen J (2000) *Molecular Electronic-Structure Theory*. Wiley, Berlin
24. Frenkel D, Smit B (2002) *Understanding Molecular Simulation: From Algorithms to Applications*. Elsevier (USA), San Diego
25. Perkins R, Fang H, Tong W, Welsh WJ (2003) *Environ Toxicol Chem* 22:1666
26. Roy K (2004) *Mol Diversity* 8:321
27. Hafner J, Wolverton C, Ceder G (2006) *MRS Res Bull* 31:659
28. Martin RM (2004) *Electronic Structure: Basic Theory and Practical Methods*. Cambridge University Press, Cambridge
29. Gavezzotti A (2002) *Cryst Eng Comm* 4:343
30. Dunitz JD, Scheraga HA (2004) *Proc Natl Acad Sci USA* 101:14309
31. Rice BM (2003) *Applications of theoretical chemistry in assessing energetic materials for performance or sensitivity*. In: Thompson DL, Brill TB, Shaw RW (eds) *Overviews of Recent Research in Energetic Materials*. World Scientific, Singapore, London, Hong Kong, New Jersey
32. Day GM, Motherwell WDS, Ammon HL, Boerrigter SXM, Della Valle RG, Venuti E, Dzyabchenko A, Dunitz JD, Scheweizer B, van Eijck BP, Erk P, Facelli JC, Bazterra VE, Ferraro MB, Hoffman DWM, Leusen FJJ, Liang C, Pantelides CC, Karamertzanis L, Price SL, Lewis TC, Nowell H, Torrisi A, Scheraga HA, Arnautova YA, Schmidt MU, aVerwer P (2005) *Acta Crystallogr, Sect B: Struct Sci* 61:511

33. Holden JR, Du Z, Ammon HL (1993) *J Comput Chem* 14:422
34. Rice BM, Sorescu DC (2006) *J Phys Chem B* 108:17730
35. Klapötke TM, University of Munich, private communication
36. Ammon HL, Maryland U, private communication
37. Karelson M, Perkson A (1999) *Comput Chem (Oxford)* 23:49
38. Dunitz JD, Filippini G, Gavezotti A (2000) *Tetrahedron* 56:6595
39. Bouhmaida N, Ghermani NE (2005) *J Chem Phys* 122:114101
40. Pan J-F, Lee Y-W (2004) *Phys Chem Chem Phys* 6:471
41. Hofmann DWM (2002) *Acta Crystallogr, Sect B: Struct Sci* 57:489
42. Cho SG, Goh EM, Kim JK (2001) *Bull Korean Chem Soc* 22:775
43. Immirzi A, Perini B (1977) *Acta Crystal A* 33:216
44. Murray JS, Brinck T, Politzer P (1996) *Chem Phys* 204:289
45. Jalbout AF, Zouh ZY, Li X, Solimannedjad M, Ma Y (2003) *J Mol Struct (THEOCHEM)* 15:664–665
46. Allen FH (2002) *Acta Crystallogr, Sect B: Struct Sci* 58:380
47. Ammon HL, Mitchell S (1998) *Propellants, Explos, Pyrotech* 23:260
48. Ammon HL (2001) *Struct Chem* 12:205
49. Politzer P, Murray JS, Brinck T, Lane P (1994) *Immunoanalysis of Agrochemicals*. In: Nelson JO, Karu AE, Wong RB (eds) *ACS Symposium Series* 586. American Chemical Society, Washington DC, p 109
50. Murray JS, Politzer P (1994) *Quantitative Treatment of Solute/Solvent Interactions*. In: Politzer P, Murray JS (eds) *Theoretical and Computational Chemistry*. Elsevier Scientific, Amsterdam, p 243
51. Murray JS, Brinck T, Lane P, Paulsen K, Politzer P (1994) *J Mol Struct (THEOCHEM)* 307:55
52. Bader RWF, Carroll MT, Cheeseman JR, Change C (1987) *J Am Chem Soc* 109:7968
53. Beaucamp S, Marchet N, Mathieu D, Agafonov V (2003) *Acta Crystallogr, Sect B: Struct Sci* 59:498
54. Trohalaki S, Pachter R, Drake GW, Hawkins T (2005) *Energy Fuel* 19:279
55. van Eijck BP, Kroon J (2000) *Acta Crystallogr, Sect B: Struct Sci* 56:535, (erratum 56:745)
56. Schmidt MW, Gordon MS, Boatz JA (2005) *J Phys Chem A* 109:7285
57. Zorn DD, Boatz JA, Gordon MS (2006) *J Phys Chem B* 110:11110
58. Jenkins HDB, Roobottom HK, Passmore J, Glasser L (1999) *Inorg Chem* 38:3609
59. Wu X, Vargas MC, Nayak S, Lotrich V, Scoles G (2001) *J Chem Phys* 115:8748
60. Reimers JR, Cai Z-L, Bilic A, Hush NS (2003) *Ann NY Acad Sci* 1006:235
61. Sukhachev DV, Pivina TS, Volk FS (1994) *Propellants, Explos, Pyrotech* 19:159
62. Muthurajan H, Sivabalan R, Talawar MB, Anniyappan M, Venugopalan S (2006) *J Hazard Mater* 133:30
63. Keshavarz MH (2005) *Thermochim Acta* 428:95
64. Keshavarz MH (2005) *J Hazard Mater* 119:25
65. Atkins PW (1982) *Physical Chemistry*. Oxford University Press, Oxford
66. Politzer P, Lane P, Concha MC (2003) *Computational Approaches to Heats of Formation*. In: Politzer PA, Murray JS (eds) *Energetic Materials: Part 1. Decomposition, Crystal and Molecular Properties (Theoretical and Computational Chemistry)*. Elsevier Science, Amsterdam, p 247
67. Byrd EFC, Rice BM (2006) *J Phys Chem A* 110:1005
68. Rice BM, Pai SV, Hare J (1999) *Combust Flame* 118:445
69. Habibollahzadeh D, Grice ME, Concha MC, Murray JS, Politzer P (1995) *J Comput Chem* 16:654

70. Politzer P, Lane P, Concha MC (2004) *Struct Chem* 15:469
71. Mathieu D, Simonetti P (2002) *Thermochim Acta* 384:369
72. Raghavachari K, Curtiss LA (2005) G2, G3 and Associated Quantum Chemical Models for Accurate Theoretical Thermochemistry. In: Dykstra CE (ed) *Theory and Applications of Computational Chemistry: The First Forty Years*. Elsevier BV, Amsterdam, p 785
73. Kim CK, Lee KA, Hyun KH, Park HJ, Kwack IY, Kim CK, Lee HW, Lee B-S (2004) *J Comput Chem* 25:2073
74. Politzer P, Murray JS, Grice ME, Desalvo M, Miller E (1997) *Mol Phys* 91:923
75. Mathieu D, Bougrat P (1999) *Chem Phys Lett* 303:601
76. Politzer P, Ma Y, Lane P, Concha MC (2005) *Int J Quantum Chem* 105:341
77. Curtiss LA, Raghavachari K (2002) *Theor Chem Acc* 108:61
78. Curtiss LA, Redfern PC, Raghavachari K, Rassolov V, Pople JA (1999) *J Chem Phys* 110:4703
79. Baboul AG, Curtiss LA, Redfern PC, Raghavachari K (1999) *J Chem Phys* 110:7650
80. Curtiss LA, Raghavachari K, Redfern PC, Rassolov V, Pople JA (1998) *J Chem Phys* 109:7764
81. Beaucamp S, Bernand-Mantel A, Mathieu D, Agafonov V (2004) *Mol Phys* 102:253
82. Rousseau E, Mathieu D (2000) *J Comp Chem* 21:367
83. Hehre WJ, Ditchfield R, Radom L, Pople JA (1970) *J Am Chem Soc* 92:4796
84. Raghavachari K, Stefanov BB, Curtiss LA (1979) *J Chem Phys* 106:6764
85. Audoux J, Beaucamp S, Mathieu D, Poullain D, Agafonov V, Allouchi H (2004) *Proceedings of the 35th International Annual Conference of ICT*, p 33/1
86. Beaucamp S, Mathieu D, Agafonov V (2005) *J Phys Chem B* 109:16469
87. Kapustinskii AF (1956) *Q Rev, Chem Soc* 10:283
88. Liu D, Zhang S, Wu Z (2003) *Inorg Chem* 42:2465
89. Glasser L (1995) *Inorg Chem* 34:4935
90. Politzer P, Murray JS (1998) *J Phys Chem A* 102:1018
91. Jenkins HDB, Tudela D, Aglasser L (2002) *Inorg Chem* 41:2364
92. Jenkins HDB (1998) In: Lide DR (ed) *Handbook of Chemistry and Physics*, 79th ed. CRC Press, Boca Raton, p 1222
93. Curtiss LA, Raghavachari K, Trucks GW, Pople JA (1991) *J Chem Phys* 94:7221
94. Mathur KC, Chauhan UK, Shrivastava R, Khadikar PV (2001) *Orient J Chem* 17:253
95. Rendic S, Jurisic B, Medic-Saric MM (1995) Biological and environmental properties of nitro-, nitramine- and nitrate compounds: Explosives and drugs application of QSPR and QSAR studies in environmental toxicology assessment. In: Richardson M (ed) *Environmental Toxicology Assessment*. Taylor & Francis, London, p 303
96. Nikolic S, Medic-Saric M, Rendic S, Trinajstic N (1994) *Drug Metabol Rev* 26:717
97. Karmarkar S, Saxena A, Verma RG, Ramendra G, Karmarkar S, Mathur K, Mathur S, Singh S, Khadikar P (2000) *Pollution Res* 19:337
98. Khadikar PV, Lukovits I, Agrawal VK, Shrivastava S, Jaiswal M, Gutman I, Karmarkar S, Shrivastava A (2003) *Indian J Chem, Sect A: Inorg, Bio-inorg, Phys, Theor* 42:1436
99. Mathur KC, Khadikar PV, Chauhan UK, Shrivastava R (2001) *Res J Chem Environ* 5:68
100. Cenas N, Nemeikaite-Ceniene A, Sergediene E, Nivinskas H, Anusevicius Z, Sarlauskas J (2001) *Biochim Biophys Acta, Gen Subj* 1528:31
101. Purohit V, Basu AK (2000) *Chem Res Toxicol* 13:673
102. Rice BM, Hare JJ (2002) *J Phys Chem A* 106:1770
103. Kamlet MJ (1976) *Proceedings 6th Symposium (International) on Detonation*, San Diego, California, p 312

104. Kamlet MJ, Adolph HG (1979) *Propellants Explos* 4:30
105. Delpuech A, Cherville J (1978) *Propellants Explos* 3:169
106. Delpuech A, Cherville J (1979) *Propellants Explos* 4:121
107. Delpuech A, Cherville J (1979) *Propellants Explos* 4:61
108. Adolph HG, Holden JR, Cichra DA (1981) Naval Surface Weapons Center Technical Report NSWC TR 80-495
109. Fukuyama I, Ogawa T, Miyake A (1986) *Propellants, Explos, Pyrotech* 11:140
110. Mullay J (1987) *Propellants, Explos, Pyrotech* 12:60
111. Mullay J (1987) *Propellants, Explos, Pyrotech* 12:121
112. Jain SR (1987) *Propellants, Explos, Pyrotech* 12:188
113. Fried LE, Ruggiero AJ (1994) *J Phys Chem* 98:9786
114. McNesby KL, Coffey CS (1997) *J Phys Chem B* 101:3097
115. Wu CJ, Fried LE (2000) *Proceedings 6th Symposium (International) on Detonation, Snowmass, Colorado*, p 490
116. Vaullerin M, Espagnacq A, Morin-Allory L (1998) *Propellants, Explos, Pyrotech* 23:237
117. Xiao H-M, Fan J-F, Gu Z-M, Dong H-S (1998) *Chem Phys* 226:15
118. Fan J, Gu Z, Xiao H, Dong H (1998) *J Phys Org Chem* 11:177
119. Fan J, Xiao H (1996) *J Mol Struct (THEOCHEM)* 365:225
120. Zhao XC, Heming X, Shulin Y (1999) *Chem Phys* 250:243
121. Belik AV, Potemkin VA, Sluka SN (1999) *Combust Explos Shock Waves* 35:562
122. Zeman S (2000) *Propellants Explos Pyrotech* 25:66
123. Owens FJ, Jayasuriya K, Abrahmsen L, Politzer P (1985) *Chem Phys Lett* 116:434
124. Murray JS, Lane P, Politzer P, Bolduc PR (1990) *Chem Phys Lett* 168:135
125. Politzer P, Murray JS, Lane P, Sjoberg P, Adolph HG (1991) *Chem Phys Lett* 181:78
126. Murray JS, Lane P, Politzer P (1995) *Mol Phys* 85:1
127. Murray JS, Lane P, Politzer P (1998) *Mol Phys* 93:187
128. Politzer P, Alper HE (1999) *Comput Chem (Singapore)* 4:271
129. Owens FJ (1996) *J Mol Struct (THEOCHEM)* 370:11
130. Politzer P, Murray JS (1996) *J Mol Struct* 376:419
131. Politzer P, Murray JS (1995) *Mol Phys* 86:251
132. Politzer P, Murray JS (1996) In: Marinkas PL (ed) *Organic Energetic Compounds*. Nova Science Publishers, Inc, New York
133. Sundararajan R, Jain SR (1983) *Ind J Technol* 21:474
134. Afanas'ev GT, Pivina TS, Sukhachev DV (1993) *Propellants Explos Pyrotech* 18:309
135. Nefati H, Diawara B, Legendre JJ (1993) *SAR QSAR Environ Res* 1:131
136. Litvinov BV, Solkan VN, Fainzilberg AA, Garmasheva NV, Loboyko BG (1995) *Dokl Akad Nauk* 341:487
137. Lin Q, Xia X, Yang G, Zhang G, Liao H (1999) *Gaoya Wuli Xuebao* 3:64
138. McCormack J, Norton ES, Scullion HJ (1969) *Explosivstoffe* 17:225
139. Zanirato P (2006) *Chim Ind (Milan, Italy)* 88:130
140. Badders NR, Wei C, Aldeeb AA, Rogers WJ, Mannan MS (2006) *J Energ Mater* 24:17
141. Shu Y, Zhang C, Wang X, Zhao X (2005) Theoretical studies on the properties of some energetic materials. In: Vagenknecht J (ed) *New Trends in Research of Energetic Materials, Proceedings of the Seminar, 8th, Pardubice, Czech Republic, Apr 19-21, 2005*. University of Pardubice, Pardubice, p 779
142. Zhang C, Shu Y, Huang Y, Wang X (2005) *J Energ Mater* 23:107
143. Zhang C, Shu Y, Huang Y, Zhao X, Dong H (2005) *J Phys Chem B* 109:8978
144. Koch E-C (2005) *Propellants, Explos, Pyrotech* 30:5
145. Zeman S (2003) *Propellants, Explos, Pyrotech* 28:308

146. Zeman S, Krupka M (2003) *Propellants, Explos, Pyrotech* 28:301
147. Zeman S, Friedl Z, Huczala R (2002) Study of the impact reactivity of polynitro compounds part III. Relationship between electronic charges at nitrogen atoms of primarily split off nitro groups and impact sensitivity of some polynitro arenes. In: Vagenknecht J (ed) *New Trends in Research of Energetic Materials, Proceedings of the Seminar, 5th, Pardubice, Czech Republic, Apr. 24–25, 2002*. University of Pardubice, Pardubice, p 426
148. Zeman S, Krupka M (2002) Study of the impact reactivity of polynitro compounds part II. Impact sensitivity as a function of the intermolecular interactions. In: Vagenknecht J (ed) *New Trends in Research of Energetic Materials, Proceedings of the Seminar, 5th, Pardubice, Czech Republic, Apr 24–25, 2002*. University of Pardubice, Pardubice, p 415
149. Koshi M, Widijaja J, Kuroki Y (2001) *Kayaku Gakkaishi* 62:283
150. Lee HW, Chung K-H, Cho SG, Lee B-S, Kim CY (2006) *International Annual Conference of ICT (2006), 37th (Energetic Materials)*, p 177/1
151. Zhang C (2006) *Chem Phys* 324:547
152. Zhao Q, Zhang S, Li QS (2005) *Chem Phys Lett* 407:105
153. Pacheco-Londono LC, De la Torre-Quintana LF, Primera-Pedrozo OM, Herrera GM, Ballesteros LM, Hernandez-Rivera SP (2004) *Proceedings of SPIE-The International Society for Optical Engineering* 5403:269
154. Saraf SR, Rogers WJ, Mannan MS (2003) *J Hazard Mater* 98:15
155. Keshavarz MH, Jaafari M (2006) *Propellants, Explos, Pyrotech* 31:216
156. Keshavarz MH, Pouredal HR (2005) *J Hazard Mater* 124:27
157. Brill TB, James KJ (1993) *J Phys Chem* 97:8752
158. Brill TB (2005) Connecting molecular properties to decomposition, combustion, and explosion trends. In: Thompson DL, Brill TB, Shaw RW (eds) *Overviews of Recent Research in Energetic Materials*. World Scientific, Singapore, London, Hong Kong, New Jersey, p 1
159. Politzer P, Murray JS (2003) Sensitivity Correlations. In: Politzer PA, Murray JS (eds) *Energetic Materials, Part 2: Detonation, Combustion, Theoretical and Computational Chemistry*. Elsevier Science, Amsterdam, p 5
160. Singh RP, Verma RD, Meshri DT, Shreeve JM (2006) *Angew Chem Int Ed* 45:3584
161. Kwon O, McKee ML (2003) Polynitrogens as Promising High-Energy Density Materials: Computational Design. In: Politzer PA, Murray JS (eds) *Energetic Materials: Part 1. Decomposition, Crystal and Molecular Properties (Theoretical and Computational Chemistry)*. Elsevier Science, Amsterdam, p 405
162. Nguyen MT (2003) *Coord Chem Rev* 244:93
163. Bartlett RJ, Fau S, Tobita M, Wilson K, Perera A (to be published)
164. Li PC, Guan J, Li S, Qian SL, Wen GX (2003) *Phys Chem Chem Phys* 5:1116
165. Cheng L, Li Q, Xu W, Zhan S (2003) *J Molec Model* 9:99
166. Liu YD, Yiu PG, Guan J, Li QS (2002) *J Mol Struct (THEOCHEM)* 588:37
167. Zhou H, Wong N-B, Zhou G, Tian A (2006) *J Phys Chem A* 110:7441
168. Zhou H, Wong N-B, Zhou G, Tian A (2006) *J Phys Chem A* 110:3845
169. Zhou G, Pu X-M, Wong N-B, Tian A, Zhou H (2006) *J Phys Chem A* 110:4107
170. Wang LJ, Zgierski MZ (2003) *Chem Phys Lett* 376:698
171. Strout DL (2005) *J Phys Chem A* 109:1478
172. Bruney LY, Bledson TM, Strout DL (2003) *Inorg Chem* 42:8117
173. Strout DL (2004) *J Phys Chem A* 108:10911
174. Sturdivant SE, Nelson FA, Strout DL (2004) *J Phys Chem A* 108:7087
175. Strout DL (2004) *J Phys Chem A* 108:2555

176. Strout DL (2006) *J Phys Chem A* 110:7228
177. Wang JL, Lushington GH, Mezey PG (2006) *J Chem Inf Model* 46:1965
178. Wang L, Mezey PG (2005) *J Phys Chem A* 109:3241
179. Zhao JF, Li QS (2003) *Chem Phys Lett* 368:12
180. Wang LJ, Mezey PG, Zgierski MZ (2004) *Chem Phys Lett* 391:338
181. Li QS, Zhao JF (2002) *J Phys Chem A* 106:5367
182. Wang LJ, Warburton P, Mezey PJ (2002) *J Phys Chem A* 106:2748
183. Dixon DA, Feller D, Christe KO, Wilson WW, Vij A, Vij V, Jenkins HDB, Olson RM, Gordon MS (2004) *J Am Chem Soc* 126:834
184. Wilson KJ, Perera SA, Bartlett RJ, Watts JD (2001) *J Phys Chem A* 105:7693
185. Cottrell R, Jones J, Gilchrist A, Shields D, Strout DL (2006) *J Phys Chem A* 110:9011
186. Strout DL (2006) *J Phys Chem A* 110:4089
187. Colvin KD, Cottrell R, Strout DL (2006) *J Chem Theory Comput* 2:25
188. Colvin KD, Strout DL (2005) *J Phys Chem A* 109:8011
189. Strout DL (2005) *J Chem Theory Comput* 1:561
190. Bruney LY, Strout DL (2003) *J Phys Chem A* 107:5840
191. Strout DL (2003) *J Phys Chem A* 107:1647
192. Wang X, Tian A-M, Wong NB, Law C-K, Li W-K (2001) *Chem Phys Lett* 338:367
193. Reichlin R, Schiferl D, Martin S, Vanderborgh C, Mills RL (1985) *Phys Rev Lett* 55:1464
194. Mills RL, Olinger B, Cromer DT (1986) *J Chem Phys* 84:2837
195. Schuch AF, Mills RL (1970) *J Chem Phys* 52:6000
196. Bini R, Ulivi L, Kreutz J, Jodl HJ (2000) *J Chem Phys* 112:8522
197. Olijnyk H, Jephcoat AP (1999) *Phys Rev Lett* 83:332
198. Olijnyk H (1990) *J Chem Phys* 93:8968
199. Goncharov AF, Gregoryanz EA, Mao HK, Liu Z, Hemley RJ (2000) *Phys Rev Lett* 85:1262
200. Eremets MI, Hemley RJ, Mao HK, Gregoryanz E (2001) *Nature* 411:170
201. Gregoryanz E, Goncharov AF, Hemley RJ, Mao H (2001) *Phys Rev B* 64:52103
202. Gregoryanz E, Goncharov AF, Hemley RJ, Mao H, Somayazulu M, Shen G (2002) *Phys Rev B* 66:224108
203. Eremets MI, Gavriluk AG, Trojan IA, Dzivenko DA, Boehler R (2004) *Nat Mater* 3:558
204. LeSar R (1984) *J Chem Phys* 81:5104
205. Mitas L, Martin RM (1994) *Phys Rev Lett* 72:2438
206. Lewis SP, Cohen ML (1992) *Phys Rev B* 46:11117
207. Mailhot C, Yang LH, McMahan AK (1992) *Phys Rev B* 46:14419
208. McMahan AK, LeSar R (1985) *Phys Rev Lett* 54:1929
209. Martin RM, Needs RJ (1986) *Phys Rev B* 34:5082
210. Mattson WD, Sanchez-Portal D, Chiesa S, Martin RM (2004) *Phys Rev Lett* 93:125501
211. Barbee III TW (1994) In: Schmidt SC et al. (ed) *In High-Pressure Science and Technology – 1993*, AIP Conf Proc No 309. AIP, New York, p 163
212. Yu HL, Yang GW, Yan XH, Xiao Y, Mao YL, Yang YR, Cheng NX (2006) *Phys Rev B* 73:012101
213. Alemany MMG, Martins JL (2003) *Phys Rev B* 68:024110
214. Mattson WD (2003) *The Complex Behavior of Nitrogen Under Pressure: Ab Initio Simulation of the Properties of Structure and Shock Waves*, Thesis, Univ Illinois at Urbana-Champaign, Urbana-Champaign
215. Kittel C (1996) *Introduction to Solid State Physics*. Wiley, New York

216. Kometani S, Eremets M, Shimizu K, Kobayashi M, Amaya K (1997) *J Phys Soc Jpn* 66:2564
217. Struzhkin VV, Hemley RJ, Mao HK, Timofeev YA (1997) *Nature* 390:382
218. Gregoryanz E, Struzhkin VV, Hemley RJ, Eremets MI, Mao H-K, Timofeev YA (2002) *Phys Rev B* 65:064504
219. Zakharov O, Cohen ML (1995) *Phys Rev B* 52:12 572
220. Vogler A, Wright RE, Kunkely H (1980) *Angew Chem Int Ed* 19:717
221. Ciezak JA (2006) US Army Research Laboratory, private communication
222. Hemley RJ (2002) The Carnegie Institution Geophysical Laboratory, private communication
223. Huynh MHV, Hiskey MA, Chavez DE, Naud DL, Gilardi RD (2005) *J Am Chem Soc* 127:12537
224. Hammerl A, Holl G, Klapötke TM, Mayer P, Noth H, Piotrowski H, Warchhold M (2002) *Eur J Inorg Chem* 4:834
225. Hang M, Huynh V, Hiskey MA, Archuleta JG, Roemer EL, Gilardi R (2004) *Angew Chem Int Ed* 43:5658
226. Patra S, Sarkar B, Ghumaan S, Fiedler J, Kaim W, Lahiri GK (2004) *Inorg Chem* 43:6108